Atmospheric
Chemistry
and Physics
Discussions

EGU Open Access

Variation in Global Chemical Composition of PM$_{2.5}$: Emerging Results from SPARTAN

Graydon Snider[1], Crystal L. Weagle[2], Kalaivani K. Murdymootoo[1], Amanda Ring[1], Yvonne Ritchie[1], Ainsley Walsh[1], Clement Akoshile[3], Nguyen Xuan Anh[4], Jeff Brook[5], Fatimah D. Qonitan[6], Jinlu Dong[7], Derek Griffith[8], Kebin He[7], Brent N. Holben[9], Ralph Kahn[9], Nofel Lagrosas[10], Puji Lestari[6], Zongwei Ma[11], Amit Misra[12], Eduardo J. Quel[13], Abdus Salam[14], Bret Schichtel[15], Lior Segev[16], S.N. Tripathi[12], Chien Wang[17], Chao Yu[18], Qiang Zhang[7], Yuxuan Zhang[7], Michael Brauer[19], Aaron Cohen[20], Mark D. Gibson[21], Yang Liu[18], J. Vanderlei Martins[22], Yinon Rudich[16], Randall V. Martin*[1,2,23]

*Corresponding author email: graydon.snider@dal.ca or randall.martin@dal.ca phone: 902-494-1820, fax: 902-494-5191

Affiliations
[1]Department of Physics and Atmospheric Science, Dalhousie University, Halifax, Canada
[2]Department of Chemistry, Dalhousie University, Halifax, Canada
[3]Department of Physics, University of Ilorin, Ilorin, Nigeria
[4]Institute of Geophysics, Vietnam Academy of Science and Technology, Hanoi, Vietnam
[5]Department of Public Health Sciences, University of Toronto, Toronto, Ontario, Canada M5S 1A8
[6] Faculty of Civil and Environmental Engineering, ITB, JL. Ganesha No.10, Bandung 40132, Indonesia
[7]Center for Earth System Science, Tsinghua University, Beijing, China
[8]Council for Scientific and Industrial Research (CSIR), Pretoria, South Africa
[9]Earth Science Division, NASA Goddard Space Flight Center, Greenbelt, Maryland, USA
[10]Manila Observatory, Ateneo de Manila University campus, Quezon City, Philippines
[11] School of Environment, Nanjing University, Nanjing, China.
[12] Center for Environmental Science and Engineering, Indian Institute of Technology Kanpur, India
[13]UNIDEF (CITEDEF-CONICET) Juan B. de la Salle 4397 – B1603ALO Villa Martelli, Buenos Aires, Argentina
[14]Department of Chemistry, University of Dhaka, Dhaka - 1000, Bangladesh
[15] Cooperative Institute for Research in the Atmosphere, Colorado State, Colorado, USA
[16] Department of Earth and Planetary Sciences, Weizmann Institute, Rehovot 76100, Israel
[17] Massachusetts Institute of Technology, Cambridge, MA, 02139, USA
[18]Rollins School of Public Health, Emory University, 1518 Clifton Road NE, Atlanta, GA 30322, United States
[19]School of Population and Public Health, University of British Columbia, Vancouver, British Columbia, Canada
[20]Health Effects Institute, 101 Federal Street Suite 500, Boston, MA 02110-1817, USA
[21]Department of Process Engineering and Applied Science, Dalhousie University, Halifax, Canada,
[22]Department of Physics and Joint Center for Earth Systems Technology, University of Maryland, Baltimore County, Baltimore, Maryland, USA
[23]Harvard-Smithsonian Center for Astrophysics, Cambridge, MA 02138, USA

Atmospheric
Chemistry
and Physics
Discussions

Abstract

18   The Surface PARTiculate mAtter Network (SPARTAN) is a long-term project designed to
19 maximize the chemical and physical information obtained from filter samples collected
20 worldwide. This manuscript discusses the ongoing efforts of SPARTAN to define and quantify
21 major ions and trace metals found in aerosols. Our methods infer the spatial and temporal
22 variability of $PM_{2.5}$ in a cost-effective manner; single filters represent multi-day averaged fine
23 particulate matter ($PM_{2.5}$), while an adjacent nephelometer samples air continuously. SPARTAN
24 instruments are collocated with AERONET to better understand the relationship between
25 ground-level $PM_{2.5}$ and columnar aerosol optical depth (AOD).

27   We have examined the chemical composition of $PM_{2.5}$ at 12 globally dispersed, densely
28 populated urban locations and a site at Mammoth Cave (US) National Park used as a baseline
29 comparison. Each SPARTAN location has so far been active between the years 2013 and 2015
30 over 2 to 22 month periods. These sites have collectively gathered over 10 years of quality
31 aerosol data. The major $PM_{2.5}$ constituents across all sites (relative contribution ± SD) were
32 ammonium sulfate (20% ± 10%), crustal material (12% ± 6.2%), black carbon (11% ± 8.4%),
33 ammonium nitrate (4.0% ± 2.8%), sea salt (2.2% ± 1.5%), trace element oxides (0.9% ± 0.6%),
34 water (7.2% ± 3.1%) and residue materials (43% ± 25%).

36   Analysis of filter samples revealed that several $PM_{2.5}$ chemical components varied by more
37 than an order of magnitude between sites. Ammonium sulfate ranged from 1.1 µg m^{-3} (Buenos
38 Aires, Argentina) to 17 µg m^{-3} (Kanpur, India [dry season]). Ammonium nitrate ranged from 0.2
39 µg m^{-3} (Mammoth Cave, in summer) to 6.7 µg m^{-3} (Kanpur, dry season). Equivalent black
40 carbon ranged from 0.7 µg m^{-3} (Mammoth Cave) to 8 µg m^{-3} (Dhaka, Bangladesh and Kanpur).
41 Comparison with coincident measurements from the IMPROVE network at Mammoth Cave
42 yielded a high degree of consistency for daily $PM_{2.5}$ ($r^2 = 0.76$, slope = 1.12), daily sulfate ($r^2 =$
43 0.86, slope = 1.03) and mean fractions of all major $PM_{2.5}$ components (within 6%). Major ions
44 generally agree well with previous studies at the same urban locations (e.g. sulfate fractions
45 agree within 4% for eight out of 11 collocation comparisons). Enhanced anthropogenic dust
46 fractions in large urban areas (e.g. Singapore, Kanpur, Hanoi and Dhaka) were apparent from
47 high Zn:Al ratios.

49   The expected water contribution to aerosols was calculated via the hygroscopicity parameter
50 κ_v for each filter. Mean aggregate values ranged from 0.15 (Manila and Ilorin) to 0.31 (Rehovot;
51 with the latter included a major sulfate event. The all-site parameter mean is 0.19. Chemical
52 composition and water retention in each filter measurement allowed inference of hourly $PM_{2.5}$ at
53 35% relative humidity by merging with nephelometer measurements. These hourly $PM_{2.5}$
54 estimates compare favorably with a beta attenuation monitor (MetOne) at the nearby US
55 embassy in Beijing, with a coefficient of variation $r^2 = 0.67$ ($n = 3167$), compared to $r^2 = 0.62$
56 when κ_v was not considered. SPARTAN continues to provide an open-access database of $PM_{2.5}$
57 compositional filter information and hourly mass collected from a global federation of
58 instruments.

1. Introduction

Fine particulate matter with a median aerodynamic diameter less than, or equal to, 2.5 μm ($PM_{2.5}$), is a robust indicator of premature mortality (Chen et al., 2008; Laden et al., 2006). Research on long-term exposure to ambient $PM_{2.5}$ has documented serious adverse health effects, including increased mortality from chronic cardiovascular disease, respiratory disease, and lung cancer (WHO, 2005). Outdoor fine particulate matter ($PM_{2.5}$) is recognized as a significant air pollutant, with an Air Quality Guideline set by the WHO at 10 μg m^{-3} annual average (WHO, 2006). Many regions of the world far exceed these long-term recommendations (Brauer et al., 2015; van Donkelaar et al., 2015), and the impact on health is substantial. The 2013 Global Burden of Disease estimated that outdoor $PM_{2.5}$ caused 2.9 million deaths (3 % of all deaths) and 70 million years of lost healthy life on a global scale (Forouzanfar et al., 2015). Atmospheric aerosol are also the most uncertain agent contributing to radiative forcing of climate change (IPCC, 2013). Aerosol mass and composition also play a critical role in atmospheric visibility (Malm et al. 1994). Additional observations are needed to improve the concentration estimates for $PM_{2.5}$ as global risk factor, and to better understand the chemical components and sources contributing to its formation.

Ground-based observations of $PM_{2.5}$ have insufficient coverage at the global scale to provide assessment of long-term human exposure. Furthermore, no global $PM_{2.5}$ protocol exists for relative humidity (RH) filter equilibration. The U.S. EPA measurements are between 30-40% RH, European measurements are below 50% RH, and different protocols exist elsewhere. Satellite remote sensing offers a promising means of providing an extended temporal record to estimate population exposure to $PM_{2.5}$ on a global scale, and especially for areas with limited ground-level $PM_{2.5}$ measurements (Brauer et al., 2015; van Donkelaar et al., 2015). Even in areas where monitor density is high, satellite-based estimates provide additional useful information on spatial and temporal patterns in air pollution (Kloog et al., 2011, 2013; Lee et al., 2012). However, there are outstanding questions about the accuracy and precision with which ground-level aerosol mass concentrations can be inferred from satellite remote sensing. Standardized $PM_{2.5}$ measurements, collocated with ground-based measurements of aerosol optical depth, are needed to evaluate and improve $PM_{2.5}$ estimates from satellite remote sensing.

Ambient humidity affects the relationship of dry $PM_{2.5}$ with satellite observations of aerosol optical depth. Aerosol water also influences the relationship between dry $PM_{2.5}$ and aerosol scatter. A large body of literature has examined the relationship of aerosol composition with hygroscopicity (e.g. IMPROVE (Hand et al., 2012; IMPROVE, 2015), CSN (Chu, 2004; USEPA, 2015), ISORROPIA (Fountoukis and Nenes, 2007), AIM (Wexler and Clegg, 2002)). More recently Petters and Kreidenweis (2007, 2008, 2013) have developed κ-Kohler theory that assigns individual κ values to all major components, from insoluble crustal materials to sea-salt. Mixed values can then be weighted by local aerosol composition.

The chemical composition of $PM_{2.5}$ also offers valuable information to identify the contributions of specific sources, and to understand aerosol properties and processes that could affect health, climate and atmospheric conditions. Spatial mapping of aerosol type using satellite observations and chemical transport modelling can help elucidate the global exposure burden of fine particulate matter composition (Kahn and Gaitley, 2015; Lelieveld et al., 2015; Patadia et

Atmospheric
Chemistry
and Physics
Discussions

107   al., 2013; Philip et al., 2014a), however ground-level sampling remains necessary to evaluate
108   these estimates and provide quantitative detail. Furthermore, the long-term health impacts of
109   specific chemical components are not well understood (e.g. Lepeule et al., 2012). There is
110   insufficient long-term $PM_{2.5}$ characterization information for adequate health impact assessments
111   of specific aerosol mixtures (e.g. Bell et al., 2007). Urban $PM_{2.5}$ speciation has been conducted in
112   North America (Hand et al., 2012) and Europe (Putaud et al., 2004, 2010), however there
113   remains need for a global network that consistently measures $PM_{2.5}$ chemical composition in
114   densely populated regions.

115
116   To meet these sampling needs, the ground-based network SPARTAN (Surface
117   PARTiculate mAtter Network) is designed to evaluate and enhance satellite-based estimates of
118    $PM_{2.5}$ by measuring fine particle aerosol concentrations and composition continuously over
119   multi-year periods at sites where aerosol optical depth is also measured (Holben et al., 1998;
120   Snider et al., 2015). The network includes air filter sampling and nephelometers that together
121   provide long-term and hourly $PM_{2.5}$ estimates at low RH (35%).

122
123   We discuss the ongoing efforts of the SPARTAN project to quantify major ions and trace
124   metals found in aerosols worldwide. Section 2 describes the methodology used to infer $PM_{2.5}$
125   composition. Section 3 describes the implementation of sub-saturated κ-Kohler theory to
126   estimate aerosol water content based on aerosol compositional information. Section 4 defines
127   crustal and residue material, black carbon, ammonium nitrate, ammonium sulfate, sea salt, and
128   trace metal oxides as a function of chemical speciation. Relative aerosol composition is
129   compared with that reported in available literature to assess the general consistency of our
130   findings. Section 5 evaluates hourly $PM_{2.5}$ estimates (35% RH) at Beijing with a beta attenuation
131   monitor at the US Embassy.

132
133   ## 2. Methodology

134
135   SPARTAN has been collecting $PM_{2.5}$ on PTFE filters for at least four months, across 13
136   SPARTAN sites. Snider et al. (2015) provides an overview of the SPARTAN $PM_{2.5}$ observation
137   network, the cost-effective sampling methods employed and post sampling instrumental methods
138   of analysis. Each site utilizes a combination of continuous monitoring by nephelometry and mass
139   concentration via filter-based sampling. Nephelometer scatter is averaged to hourly intervals at
140   three wavelengths (457nm, 520nm, 634nm), and converted to 550 nm via a fitted Angstrom
141   exponent. Total scatter is proportional to $PM_{2.5}$ mass and volume (Chow et al., 2006), hence we
142   provide dry (35% RH) hourly $PM_{2.5}$ estimates by combining scatter at 550 nm at ambient RH
143   with filter mass and chemical composition information used to determine water content as
144   described below.

145
146   Briefly, filter-based measurements are collected with an AirPhoton SS4i automated air
147   sampler. Each sampler houses a removable filter cartridge that protects seven sequentially active
148   filters plus a field blank. Air samples first pass through a bug screen and then a greased impactor
149   plate to remove particles larger than PM_{10}. Aerosols are collected in sequence on a preweighed
150   Nuclepore filter membrane (8 μm, SPI) that removes coarse-mode aerosols ($PM_{2.5-10}$), while fine
151   aerosols ($PM_{2.5}$) are then collected on pre-weighed PTFE filters (2 μm, SKC). For each filter,
152   sampling is timed at regular, staggered 24-hour intervals throughout a 9-day period. Sampling

153   ends for each filter at 9 AM when temperatures are low, to reduce loss of semi-volatile
154   components. Filters are transported inside cartridges to and from measurement sites and between
155   the central SPARTAN cleanroom and laboratory at Dalhousie University where analysis is
156   conducted.
157
158   Figure 1 shows the locations of operating SPARTAN sites across 11 countries that
159   operated within the period January 2013 to November 2015. Urban $PM_{2.5}$ concentrations at these
160   sites span an order of magnitude, from 9 µg m^{-3} (e.g. Atlanta) to nearly 100 µg m^{-3} (Kanpur).
161   Sites include a variety of geographic regions including partial desert (Ilorin, Rehovot, Kanpur),
162   coastline (Buenos Aires, Singapore), and developing megacities (Dhaka). Site locations are
163   designed to sample under a variety of conditions, including biomass burning, (e.g. West Africa
164   and South America), biofuel emissions (e.g. South Asia), monsoonal conditions (e.g. West
165   Africa and Southeast Asia), suspended mineral dust (e.g. West Africa and the Middle East) and
166   urban crustal material. Each SPARTAN site provides a representative example of local and
167   regional conditions in highly populated areas. The sites of Atlanta and Mammoth Cave are
168   included for instrument inter-comparison purposes.

169   ### 2.1. Filter weighing

170   Filters (PTFE, capillary) are both pre and post-weighed in triplicate using a Sartorius Ultramicro
171   balance with 0.1 µg precision. Weighing is performed in a cleanroom facility at 35 ± 5% RH and
172   20-23°C. A total of 437 quality-controlled filters have been weighed across all SPARTAN sites
173   (Table 3). The mean weighed collected material on each filter is 100 ± 90 µg. The combined
174   uncertainty (± 2σ) of repetitive triplicate measurements is 4.0 µg. Filters are subsequently
175   measured for surface reflectance to obtain black carbon, water-soluble ions, and trace metals.

176   ### 2.2. Equivalent Black Carbon (EBC)

177   We define the equivalent black carbon (EBC) as the black carbon content of PTFE filters derived
178   via surface reflectance R using the Diffusion Systems Smoke Stain Reflectometer EEL 43M
179   (Quincey et al., 2009) as further discussed in Sect. 4.6. We use the term equivalent black carbon
180   following the recommendation of Petzold et al. (2013) for data derived from optical absorption
181   methods.

182   ### 2.3. Trace metals

183   To maximize the information extracted from the filters, each one is cut in half with a ceramic
184   blade following approaches similar to Zhang et al. (2013) and Gibson et al. (2009). One filter
185   half is analyzed for relevant trace metals, i.e. crustal components Zn, Mg, Fe, and Al. We digest
186   this half by adding it to 3.0 mL of 7% trace metal grade nitric acid, similar to Fang et al. (2015).
187   The acid/filter combination is boiled at 97°C for 2 hours, and the liquid extract is submitted for
188   quantitative analysis via inductively coupled plasma mass spectrometry (ICP-MS, Thermo
189   Scientific X-Series 2).

190   ### 2.4. Water soluble ions

191   Water-soluble ions NO_3^-, SO_4^{2-}, NH_4^+, Na^+ are detected using the second filter half. The filter is
192   spiked with 120 µL of isopropyl alcohol and immersed in 2.9 mL of 18 MΩ Milli-Q water.
193   Filters and liquid extracts are sonicated together for 25 min before being passed through a 0.45

194 μm membrane filter to remove larger matrix components. Extractions are analyzed by ion
195 chromatography (IC) via a Thermo Dionex ICS-1100 instrument (anions) and a Thermo Dionex
196 ICS-1000 (cations) instrument (Gibson et al., 2013a, 2013b).
197

3. Aerosol hygroscopicity

199
200 We apply the single-parameter measure of aerosol hygroscopicity (κ) developed by Petters
201 and Kreidenweis (2007, 2008, 2013) to represent the contribution of water uptake by individual
202 components. The κ parameter is defined from 0 (insoluble materials) to greater than 1 for sea
203 salt. Although initially developed for supersaturated CCN conditions, hygroscopic parameters κ
204 have been more recently used in sub-saturated conditions (Chang et al., 2010; Dusek et al., 2011;
205 Giordano et al., 2013; Hersey et al., 2013). For particle diameters that dominate the mass fraction
206 of $PM_{2.5}$ (larger than 50 nm), the difference in κ between CCN and sub-saturated aerosols is
207 small (Dusek et al., 2011). The water retention of internal mixtures of aerosol components is
208 often predicted within experimental error (Kreidenweis et al., 2008). Aged, polarized organic
209 material, which is a major component of $PM_{2.5}$, shows comparable growth factors both in super-
210 and sub-saturated regions (Rickards et al., 2013).
211
212 The volume hygroscopicity parameter κ_v is defined as a function of particle volume V and
213 water activity a_w

$$\frac{1}{a_w} = 1 + \kappa_v \frac{V_d}{V_w} \qquad \text{Eq. 1}$$

214 where V_d and V_w are the dry particulate matter and water volumes, respectively. To a first-order
215 approximation $a_w = RH/100$. Aerosol volume growth is related via κ and RH by defining $f_v(RH)$
216 as the humidity-dependent ratio of wet and dry aerosol volume:

$$f_v(\text{RH}) \equiv \frac{V_{tot}}{V_d} = \frac{V_d + V_w}{V_d} = a + \kappa_v \frac{\text{RH}}{100 - \text{RH}} \qquad \text{Eq. 2}$$

217 Combining the previous equations and relating to a diameter D growth factor ($GF \equiv D/D_d$) yields

$$GF = \left(a + \kappa_v \frac{\text{RH}}{100 - \text{RH}} \right)^{1/3} \qquad \text{Eq. 3}$$

218 where $a = 1$, except for sea salt as discussed in Sect. 3.1. Reliable estimates of κ_v are available
219 for individual components (*c.f.* Table 1).
220
221 The next sections outline how we apply κ to represent mass and volume hygroscopic growth
222 in major hygroscopic aerosol components. Four species directly contribute to water uptake:
223 ammonium nitrate (ANO_3), ammonium sulfate (ASO_4), sea salt ($NaCl$), and organics. We treat
224 black carbon (EBC), crustal material (CM), and trace oxides (TEO) as non-hygroscopic. We
225 evaluated inorganic species' growth curves using the AIM model (Wexler and Clegg, 2002) for
226 RH = 10 – 90% except for sea salt, which included RH = 0%. Hygroscopic parameters were
227 matched to modeled fits. Aerosols are treated as internally mixed, without deliquescence or
228 efflorescence points, as discussed further below.

3.1. Inorganic behavior

229

230   Figure 2 shows the hygroscopic growth for inorganics. The κ_v value of 0.51 for ASO$_4$
231 best matches the AIM model over RH = 10-90% and is similar to the *GF*-derived κ_v = 0.53
232 estimated by Petters and Kreidenweis (2007). Our AIM-derived ANO$_3$ growth curve is slightly
233 smaller than ASO$_4$, at κ_v = 0.41. Although both ammonium compounds share the same *GF* = 1.6
234 at RH = 85% (Sorooshian et al., 2008), ANO$_3$ is less hygroscopic at lower RH.
235
236   Sea salt accounts for a small fraction of aerosol mass over land, however its hydrophilic
237 nature makes it significant for water retention. A 1:1 v/v with water for RH = 0% (Kreidenweis
238 et al., 2008) yields *a* = 2 (Eq. 2 and 3). A hygroscopic constant κ_v = 1.5 then best fits AIM from
239 the deliquescence point up to 90% RH.
240
241   We follow the widely used convention (e.g. IMPROVE) that PM$_{2.5}$ under variable sub-
242 saturated RH does not exhibit deliquescent phase transitions. There is compelling evidence to
243 adopt smooth hygroscopic growth curves. Various experiments show sub-micrometer, internally
244 mixed aerosols will not deliquesce as readily as pure compounds. For example, Badger et al.
245 (2006) observed ASO$_4$ aerosol deliquescence is clearly inhibited by the presence of humic acids.
246 A smooth growth curve has been observed over the range RH = 10 – 85% for ambient aerosols at
247 Jungfraujoch (Swietlicki et al., 2008). Analysis of submicron aerosol mixtures consisting of
248 NaCl, ASO$_4$, ANO$_3$, and levoglucosan also showed no apparent phase transition (Svenningsson
249 et al., 2006).

3.2. Organic matter behavior

250

251   Identifying a representative organic hygroscopic parameter is challenging, as many volume
252 growth curves are available based on a variety of laboratory experiments and field campaigns.
253 Organic composition varies by site, and by season. The Appendix table Al contains a collection
254 of hygroscopic parameters from the literature. Values for $\kappa_{v,OM}$ range from 0 to 0.2. We choose a
255 single $\kappa_{v,OM}$ value based on the oxygen/carbon ratio (O:C), which is a function of oxidation,
256 hence age of the organics. Generally O:C ratios are between 0.2 – 0.8 in urban environments
257 (Rickards et al., 2013). We select an O:C ratio of 0.5 to represent the populated nature of
258 SPARTAN sites (e.g. Robinson et al., 2013). This corresponds to an organic parameter of
259 $\kappa_{v,OM} = 0.1$ for a variety of organic mixtures (Jimenez et al., 2009).

3.3. Aerosol water in multi-component systems

260

261   Mass-based hygroscopic water uptake κ_m is more convenient than κ_v to estimate water
262 retention in gravimetric analysis. The parameters κ_v and κ_m are related by water-normalized
263 density, $\kappa_{m,X} = \kappa_{v,X}/\rho_X$. Table 1 contains κ_v values identified for major aerosol chemical
264 components and densities. For a multi-component system we estimate aerosol water mass using a
265 mass-weighted combination of κ_m values:

$$\kappa_{m,tot} = \frac{1}{M} \sum_X m_X \kappa_{m,X}$$ Eq. 4

266   Mass calculations are used to determine residue aerosol mass as described in Sect 4.9.
267 Estimates of total water uptake by volume are applied to aerosol light scatter in Sect. 5. The

Atmospheric
Chemistry
and Physics
Discussions

268   volume parameter $\kappa_{v,tot}$ is similarly determined by a linear combination of volume-weighted
269   components X (e.g. Bezantakos et al., 2013):

$$\kappa_{v,tot} = \frac{1}{V} \sum_X v_X \kappa_{v,X} \qquad \text{Eq. 5}$$

270   The hygroscopic growth of ASO$_4$ and organic mixtures are treated as linear combinations of pure
271   compounds (Robinson et al., 2013). Errors in aerosol water uptake are less significant in mixtures
272   than for individual species due to dilution effects (Kreidenweis et al., 2008). For ambient aerosols,
273    $\kappa_{v,tot}$ usually lies between 0.14 and 0.39 (Carrico et al., 2010).
274

4. PM$_{2.5}$ aerosol composition

276
277   Section 2 defines the methodology of basic chemical species obtained in SPARTAN filters.
278   Section 4 defines the chemical assumptions made when compiled into Figure 1. Each component
279   is discussed in turn below. Table 2 contains a summary of equations and accompanying
280   references used to quantify SPARTAN PM$_{2.5}$ chemical composition.

4.1. Sea Salt

282   We take 10% of [Al] to be associated with Na and remove this crustal sodium component
283   (Remoundaki et al., 2013). Sea salt is then represented as 2.54[Na$^+$]$_{ss}$ to account for the
284   associated [Cl$^-$] (Malm et al., 1994).

4.2. Ammonium nitrate (ANO$_3$)

286   We assume that all nitrate is neutralized by ammonium as NH$_4$NO$_3$. The corresponding mass of
287   ANO$_3$ is a 1:1 molar ratio of NH$_4$:NO$_3$, or 1.29[NO$_3^-$] based on molecular weight.

4.3. Sodium sulfate (Na$_2$SO$_4$)

289   Sodium sulfate is treated as a fraction of measured sodium, 0.18[Na$^+$]; however, it contributes
290   negligibly to total aerosol mass ($< 0.1\%$) at all sites.

4.4. Ammonium sulfate (ASO$_4$)

292   Ammonium not associated with nitrate, and sulfate not associated with sodium, are assumed to
293   mutually associate as a mixture of NH$_4$HSO$_4$ and (NH$_4$)$_2$SO$_4$.

4.5. Crustal material (CM)

295   Crustal material consists of re-suspended road dust, desert dust, soil, and sand. Following the
296   elemental composition of natural dust by Wang (2015), we generalize that natural CM consists
297   of 10% [Al + Fe + Mg]. Aluminum, iron, and magnesium are chosen due to their collectively
298   consistent composition in dust (predominantly natural origin) and frequency above detection
299   limit ($> 95\%$). Silicon is not available for dust analysis. Titanium was found not to contribute
300   significantly ($< 1\%$) to CM mass.

4.6. Equivalent Black Carbon (EBC)

301
302 The amount of EBC carbon (μg) is logarithmically related to concentration, as determined by
303 relative surface reflectance R/R_0. For a given exposed filter area, absorption cross-section and
304 light path, reflectance is related to concentration via

$$[EBC] = \frac{-A}{qv} \ln\left(\frac{R}{R_0}\right) \qquad \text{Eq. 6}$$

305 where v is volume of air (0.9 to 5.8 m^3), A is the filter surface area (3.1 cm^2), and q is the product
306 of the effective reflectivity path p and mass-specific absorption cross section σ_{SSR} (cm^2/μg). The
307 absorption coefficient σ_{SSR} used here is 0.06 cm^2/μg based on prior literature (Barnard et al.,
308 2008; Bond and Bergstrom, 2006), adjusted to the 620 nm detection peak of the SSR. The
309 effective light path p here is taken to be 1.5 for our thick PTFE filters (e.g. Taha et al., 2007). We
310 treat water uptake by EBC as negligible.

4.7. Trace elemental oxides (TEO)

311
312 Trace elemental oxides are the summation of oxides for all measured ICP trace elements, and
313 make up a negligible portion of total mass (< 1%). We include these concentrations for
314 completeness while assuming negligible water uptake by TEO.

4.8. Particle-bound water (PBW) associated with inorganics

315
316 We estimate the water-mass uptake for the inorganic fraction of aerosols species sea salt (NaCl),
317 ammonium nitrate (ANO₃) and ammonium sulfate (ASO₄). The mass of particle-bound water
318 (PBW) associated with species X is

$$PBW_X = [X]\kappa_{m,X} \frac{RH}{100 - RH} \qquad \text{Eq. 7}$$

319 The total mass of inorganic (IN) PBW is then $PBW_{IN} = \sum_X PBW_X$.

4.9. Residue matter (RM)

321 Residue matter at our weighing conditions of 35 ± 5 % RH ($RM_{35\%}$) is estimated by subtracting
322 dry inorganic mass, $[IN] = \Sigma[X]$, and its associated water from $PM_{2.5}$:

$$RM_{35\%} = PM_{2.5,35\%} - [IN] - [PBW_{IN}] \qquad \text{Eq. 8}$$

323 Negative $RM_{35\%}$ values are retained if reconstructed inorganic mass at 35% RH exceeds total
324 $PM_{2.5}$ by less than 10%, otherwise values are flagged and excluded from the mass average.
325 Negative values occur, on average, 2% of the time. Water-free RM (0% RH) is estimated by
326 subtracting organic-associated PBW using an estimated hygroscopic parameter $\kappa_{m,RM} = 0.07$
327 (Table 1).

4.10. Overview of PM₂.₅ mass speciation

329 Table 3 and Figure 1 contain the resulting $PM_{2.5}$ mass and composition at SPARTAN sites.
330 The mean SPARTAN composition over all sampling sites in descending concentration is 43%
331 RM, 20% ASO₄, 12% CM, 11% EBC, 4% ANO₃, 2% NaCl and 1% TEO.
332

Atmospheric
Chemistry
and Physics
Discussions

333   There is significant variation of relative and absolute speciation from long-term averages.
334   Concentrations of $PM_{2.5}$ span an order of magnitude, from 9 µg m^{-3} (Atlanta, winter-spring) to 97
335   µg m^{-3} (Kanpur, dry season). ASO_4 concentrations range from 1 µg m^{-3} (Buenos Aires, summer)
336   to 17 µg m^{-3} (Kanpur, dry season). The fraction of sulfate in $PM_{2.5}$ exhibits much weaker spatial
337   variation (10-30%). Increases in ASO_4 coincide with increases in total $PM_{2.5}$ but less pronounced
338   fractional increases. Hence locations with enhanced sulfate sources tend to have enhancements in
339   sources of other PM components.
340
341   ANO_3 concentrations exhibit even larger spatial heterogeneity than sulfate. Absolute values
342   range from 0.2 µg m^{-3} (Mammoth Cave, summer) to above 6 µg m^{-3} (Kanpur, dry season).
343   Corresponding mass fractions are 7-8 % in Kanpur, Beijing, and Buenos Aires, and below 2% in
344   Bandung. This heterogeneity reflects large spatial and temporal variation in NH_3 and NO_x
345   sources. There were noticeable increases in ANO_3 during wintertime periods in Beijing, Kanpur,
346   and Dhaka, coinciding with lower temperatures.
347
348   CM concentrations span an order of magnitude from 0.9 µg m^{-3} (Atlanta) to 13 µg m^{-3}
349   (Beijing). The fraction of CM in $PM_{2.5}$ exhibits pronounced variation (4-24%). Except during
350   dust storms, CM does not show clear patterns of temporal or regional variation. This could be
351   explained by the significant, non-seasonal contribution from road dust. Anthropogenic dust may
352   account for over 80% of CM in regions with urban traffic and agriculture (Huang et al., 2015).
353
354   We used Zn:Al ratios to assess the relative importance of local road dust (c.f. Table 3).
355   Aluminum is mostly natural in origin (Zhang et al., 2006) whereas Zn is primarily from tire wear
356   (Begum et al., 2010; Councell et al., 2004). For example, ratios are above 2 for Dhaka and
357   Hanoi, but less than 0.5 for Ilorin, Mammoth Cave, Beijing, Atlanta, and Buenos Aires. In fine-
358   mode aerosols, the ratio tends to be highest in large cities distant from natural CM. In coarse-
359   mode aerosols, a low Zn:Al ratio (< 0.1) indicates that aerosol mass is dominated by regional
360   dust.
361
362   Of the remaining PM components, EBC is highly heterogeneous. Absolute values range from
363   0.9 µg m^{-3} (Atlanta) to 8 µg m^{-3} (Dhaka and Kanpur). Mass fractions of EBC ranged from 3%
364   (Singapore) to 24% (Manila). Trace element oxide (TEO) material is mainly composed of Zn,
365   Pb, Ni, Cu, and Ba, hence also derived mainly from anthropogenic sources. TEO contributes
366   negligibly to total mass (1%), as expected. Sea salt remains a consistently small contributor (2%)
367   to total mass, except for Buenos Aires and Rehovot (6%) due to coastal winds. Particle-bound
368   water (PBW) mass, at 35% humidity, is determined from the growth parameter κ_m (κ_v/ρ, c.f. Eq.
369   7 and Tables 1 & 2). PBW is a function of ASO_4, ANO_3, and sea salt, with a mass contribution
370   similar to EBC (7%). At low humidity the combined mass of ANO_3, EBC, TEO, sea salt, and
371   PBW account for 15-35 % of aerosol mass.
372
373   The RM fraction is implicitly understood to be the organic aerosol mass fraction. RM is
374   inferred from mass reconstruction of inorganic compounds, PBW, and total filter-weighed mass.
375   In terms of relative composition, RM spans a factor of two, from 30% mass in Buenos Aires to
376   almost 60% in Kanpur, and averages about half the total mass of $PM_{2.5}$. Temporal changes in
377   RM tend to coincide with increases in ASO_4, with an all-site $r^2 = 0.92$. Although RM is not fully
378   independent of ASO_4, this relationship may imply common sources.

Atmospheric
Chemistry
and Physics
Discussions

379
380   We also interpreted the abundance of water-soluble potassium K relative to Al as an indicator
381   of wood smoke (Munchak et al., 2011). K:Al ratios averaged over each site range from 1.4
382   (Mammoth Cave) to 19.9 (Singapore). Singapore was downwind of significant Indonesian forest
383   fire smoke during our Aug-Sept 2015 sampling period. Combustion activity is also apparent in
384   Kanpur (K:Al = 14.0), whereas Ilorin, Buenos Aires, and Atlanta show less combustion activity
385   with ratios below 3.
386
387   We investigated general compositional correlations between and within aerosol modes.
388   Coarse and fine mode mass fractions are approximately equal. The all-site mean of $PM_{2.5}/PM_{10}$
389   fraction is 0.49, with fractions ranging from below 0.40 (Hanoi, Buenos Aires, and Manila) to
390   above 0.55 (e.g. Bandung, Kanpur, Atlanta, Mammoth Cave, and Singapore). High fine-mode
391   fraction are therefore not necessarily an indicator of high absolute $PM_{2.5}$. The two modes were
392   also temporally correlated, though sometimes weakly, from $r^2 = 0.15$ (Hanoi) to $r^2 = 0.76$
393   (Rehovot). Within $PM_{2.5}$, we observe strong temporal correlations between sulfate and
394   ammonium ($r^2 = 0.72 - 0.99$). Nitrate and ammonium are less consistently related, ranging from
395   high values in Kanpur ($r^2 = 0.72$) and Beijing ($r^2 = 0.58$), to weaker values in Ilorin and Manila
396   ($r^2 = 0.11$). The strength of correlations could be influenced by excess ammonium relative to
397   sulfate. The $[NH_4^+]/[SO_4^{2-}]$ ratio in $PM_{2.5}$ is 2.6 in Kanpur and 1.3 in Ilorin.

398   ### 4.11.   Collocation overview

399   We compare SPARTAN $PM_{2.5}$ speciation with previous measurements available from the
400   literature, focusing on relative $PM_{2.5}$ composition of major species from collocated studies within
401   the last 10 years. TEO is omitted due to lack of significant mass contribution. Aerosol water
402   content is also omitted as it was not directly measured in any of these collocation studies. If not
403   provided, CM is treated as defined in Sect 4.5 where possible. Organic mass (OM) to organic
404   carbon (OC) ratios are from Philip et al. (2014b) with updates from Canagaratna et al. (2015).
405
406   Figure 3 provides an overview of the comparison studies organized by SPARTAN data
407   availability. Only sampling at Mammoth Cave sampling was temporally coincident with the
408   comparison data. SPARTAN compositional information is generally consistent with previous
409   studies, considering inter-annual chemical variation and measurement uncertainty. For example,
410   both SPARTAN and comparative studies find that $PM_{2.5}$ is composed of between 10-30% ASO_4
411   and 5-20% CM for all sites. SPARTAN EBC mass fraction generally matches within 5
412   percentage points of collocated studies, except for Bandung and Kanpur. SPARTAN and prior
413   studies find that ANO_3 is usually a small fraction of total mass, except at Beijing and Kanpur
414   (7%) due to their high agricultural and industrial activity. All studies find that sea-salt is below
415   3% of total mass. SPARTAN-derived RM has potentially the largest potential error, yet typically
416   is consistent with the combined organic and unknown masses of other studies. SPARTAN
417   measurements support the expectation that RM is predominantly organic.
418
419   Below we discuss each site in more detail. We also examined how our chemical composition
420   from a global array of sites relate to local anthropogenic activities and surrounding area.
421   References to land type at specific sites are derived from Latham et al. (2014), unless otherwise
422   indicated.
423

Atmospheric
Chemistry
and Physics
Discussions

424

4.12.   Individual site characteristics

426 ***4.12.1 Beijing, China (n = 100)***
427   Beijing has attracted considerable attention for its air pollution (Chen et al., 2013).
428 Agricultural areas to the west and the Gobi Desert to the north surround the city's 19 million
429 dwellers. The SPARTAN air sampler is located on the Tsinghua University campus, 15 km from
430 the downtown center. This is our longest-running site, with over two years of near-continuous
431 sampling to date. It reports the third-highest $PM_{2.5}$, at 69 µg m^{-3}, the third highest ASO_4 (12 µg
432 m^{-3}) and the highest CM (13 µg m^{-3}) of all sites. The high ANO_3 (4.7 µg m^{-3}) reflects significant
433 urban NO_x near agricultural NH_3 sources. ANO_3 values were highest during winter, as expected
434 from ammonium-nitrate thermodynamics. A high CM component in the springtime reflects
435 regional, natural CM sources. The mean $PM_{2.5}$ Zn:Al ratio is lower than other large cities (0.45)
436 likely due to significant natural dust sources. The lowest coarse-mode Zn:Al mass ratios are
437 observed in April 2014 (0.07) and April 2015 (0.06) during the annual Yellow dust storm season.
438 This is balanced by urban dust sources, in agreement with Lin et al. (2015) who found high CM
439 in industrial areas of Beijing.

440

441   *Beijing Comparison:* Relative masses in Beijing compare well with previous studies.
442   SPARTAN ASO_4 (19%) is close to Yang et al. (2011) (17%) and Oanh et al. (2006) (20%)
443   and the RM of 42% was similar to their combined OM (33 and 29%) and unknown fractions
444   (10 and 24%). SPARTAN ANO_3 concentrations (7%) are lower than either previous study
445   (11-12 %), possibly due to volatilization losses, but still relatively large. CM is comparable
446   to Yang et al. (2011) (21% vs. 19%), but higher than Oanh et al. (2006) (5%), potentially due
447   to different definitions.

448

449 ***4.12.2 Bandung, Indonesia (n = 71)***
450   Bandung is located inland on western Java surrounded by a volcanic mountain range and
451 agriculture (e.g. tea plantations). The sampler is located on the ITB campus, 5 km north of the
452 city center. Almost two years of sampling have resulted in a mean $PM_{2.5}$ concentration of 31 µg
453 m^{-3}. Sea salt is low at this elevated (826 m) inland site. ANO_3 and CM levels are also low, but
454 RM is moderately high compared with other sites, at 51%, which could be explained by large
455 amounts of vegetative burning. Organic $PM_{2.5}$ mass fractions can rise above 70% during
456 combustion episodes (Fujii et al., 2014). Volcanic sources of sulfur, in addition to industrial
457 sources, may explain the relatively higher ASO_4 compared with Manila or Dhaka (Lestari and
458 Mauliadi, 2009). Influxes of volcanic dust from the Sinabang volcano from August – September
459 2014 (2000 km northwest of Bandung) could explain why coarse-mode Zn:Al ratios drop to 0.09
460 for this period compared to the annual mean coarse-mode ratio of 0.21.

461

462   *Bandung Collocation:* Bandung is a volcanically active area, so that composition, in
463   particular ASO_4, differs due to naturally variable circumstances. SPARTAN ASO_4 (20%) is
464   higher than Lestari and Mauliadi (2009) (4%) while more consistent with Oanh et al. (2006).
465   SPARTAN EBC (14%) is less than either previous study (19% and 25%) and the more recent
466   analysis of 19% BC (Santoso et al., 2013). SPARTAN ANO_3 is less than 2% relative mass,
467   lower than measured by Oanh et al. (2006) (13%) but similar to Lestari and Mauliadi (2009).

Atmospheric
Chemistry
and Physics
Discussions

468   Both of the earlier studies show lower RM fractions (36%, and 42%) compared with our 54%
469   RM.
470
471   ### 4.12.3 Manila, Philippines (n = 56)
472   Manila is a coastal city located in Manila Bay, adjacent to the South China Sea and
473   surrounded by mountains. The sampling station, located at the Manila Observatory, is about 40
474   m higher in altitude than the central city. The $PM_{2.5}$ concentrations at the observatory (17 μg m^{-3})
475   are expected to be lower than in the main city, but still influenced by vehicular traffic, fuel
476   combustion and industry (Cohen et al., 2009). Compared to the all-site average, the CM fraction
477   in Manila is typical (11%), but black carbon is twice as great (25%). The high EBC agrees with
478   previous observations, attributable to a relatively high use of diesel engines (Cohen et al., 2002).
479
480   *Manila Collocation:* SPARTAN fractions of ASO_4 and EBC are similar to Cohen et al.
481   (2009). Our RM (44%) is lower than OM (57%), whereas SPARTAN CM was greater than
482   Cohen et al. (2009). These differences could reflect sampling differences, or emission
483   changes over the last decade.
484
485   ### 4.12.4 Dhaka, Bangladesh (n = 41)
486   Dhaka is a densely populated city (17,000 persons/km^2) in a densely populated country
487   (1,100 persons/km^2). The sampler is situated in the heart of downtown Dhaka, on the University
488   of Dhaka rooftop, and is influenced by air masses from the Indo Gangetic Plain (Begum et al.,
489   2012). More than half the country is used for agricultural purposes (Ahmed, 2013). Local
490   contributing $PM_{2.5}$ sources include coal and biomass burning, and heavy road traffic combustion
491   products and dust (Begum et al., 2010, 2012). $PM_{2.5}$ concentrations are the fourth highest of any
492   SPARTAN site, at 52 μg m^{-3}. Dhaka has the second-highest absolute EBC of any site, at 8.0 μg
493   m^{-3}. A high EBC can be explained by the abundance of truck diesel engines (Begum et al.,
494   2012). We estimate 41% of $PM_{2.5}$ in Dhaka is RM. Crop or bush burning on both a local and
495   regional scales contribute significantly to organics (Begum et al., 2012). The high mean $PM_{2.5}$
496   Zn:Al ratio of 2.48 reflects a large contribution from urban traffic.
497
498   ### 4.12.5 Ilorin, Nigeria (n = 40)
499   Ilorin is located in a rural area with low-level agriculture and shrub vegetation; The sampler
500   is sited on the university campus, 15 km east of the city of 500,000 people. Aerosol loadings
501   have seasonal cycles from agricultural burning events and dust storms (Generoso et al., 2003).
502   The RM accounted for two thirds of total mass, among the largest, influenced by biomass
503   burning. There is evidence of biomass burning in the $PM_{2.5}$ peak in late spring 2014, and again in
504   2015. Lower ASO_4 (12%) compared to other SPARTAN sites reflects the sparse surrounding
505   industry. CM levels are comparable to other locations, except during dust storms. During a dust
506   storm (between April 14th - May 2nd 2015), CM explained 65% of total mass, 3% came from
507   combined sea salt, ANO_3 and ASO_4, leaving a significant fraction (50%) assigned to RM. The
508   PM_c Zn:Al ratio during the storm was 0.01, compared with 0.25 during non-storm days.
509
510   ### 4.12.6 Kanpur, India (n = 33)
511   Kanpur is a city of 2.5 million people. The sampler is located at the IIT Kanpur campus
512   airstrip, about 10 km northwest of the city. Kanpur lies in the Indo-Gangetic Plain, where
513   massive river floodplains are used for agricultural and industrial activity (Ram et al., 2012). We

Atmospheric
Chemistry
and Physics
Discussions

514   sampled from December 2013 – May 2014, and September-November 2014, capturing one dry
515   season. SPARTAN-measured $PM_{2.5}$ for this period was 97 µg m^{-3}, the highest of any SPARTAN
516   site, of which 55% is RM, 18% ASO_4, and 7% ANO_3. The absolute values of all three
517   components are also the highest among those measured. Molar $[NH_4^+]:[SO_4^{2-}]$ ratios are higher
518   in Kanpur (2.6) than elsewhere as well. High background ammonia has been observed in the
519   region from satellite (e.g. Clarisse et al., 2009), and would explain the high levels of ANO_3.
520   Wood smoke is apparent from the high K:Al ratio (> 10), associated with organic matter burning
521   during winter dry months. We detected significant Zn concentrations (Zn:Al = 1.4), in agreement
522   with Misra et al. (2014), who observed a tripling of zinc during pollution-sourced episodes.

524   *Kanpur Collocation:* SPARTAN $PM_{2.5}$ concentrations, as well as RM, reach a maximum
525   during the month of December. This is consistent with recent work (Villalobos et al., 2015),
526   who attribute this increase to agricultural burning and stagnant air. Relative fractions among
527   the major species CM, salt, ASO_4 & ANO_3 all match well with previous studies (Behera and
528   Sharma, 2010; Chakraborty et al., 2015; Ram et al., 2012) that also sampled during winter
529   dry seasons. Chakraborty et al. (2015) measured 70% organic mass composition and found a
530   combined mass of 28% for ASO_4 + ANO_3 compared to SPARTAN mass (26%). SPARTAN
531   ASO_4 (19%) compares well to 13% for Ram et al. (2012) and 18% for Behera and Sharma
532   (2010), and ANO_3 (7.4%) is close to previous values (6.1% and 6.6%). SPARTAN EBC is
533   slightly overestimated, by 4-6%. SPARTAN CM (5%) is lower than Behera and Sharma
534   (2010) (10%). Notably the combined OM + unknown fractions from these previous two
535   studies account for two thirds of aerosol mass, similar to our 60% RM estimate.

4.12.10 Buenos Aires, Argentina (n = 21)

538   Buenos Aires has a metropolitan population of 12 million. SPARTAN instruments are
539   located on the urban CITEDEF campus 20 km west of the central downtown. The megacity, the
540   southernmost in our study, is surrounded by grassland and farming on the west and the Atlantic
541   Ocean on the east. The latter explains the relatively high proportion (6%) of sea salt. Total $PM_{2.5}$
542   (10 µg m^{-3}) and relative RM (27%) are low compared with other large metropolitan areas, likely
543   due to clean maritime air. In addition to sea salt and natural CM, the contribution of EBC (11%),
544   which could be explained by significant local truck diesel combustion (Jasan et al., 2009).

4.12.7 Mammoth Cave NP, US (n = 19)

547   The Mammoth Cave sampling site straddles National Park mountainous terrain to the north
548   and east, with farmland to the south and west. It is about 35 km from the closest town, Bowling
549   Green, KY, with about 50,000 residents. Sources of PM are expected to be non-local, hence we
550   consider it our 'background' site.

552   *Mammoth Cave National Park Collocation*: This temporary SPARTAN site was deployed
553   for comparison with the IMPROVE network station (IMPROVE, 2015). Unique among our
554   sites, sampling was temporally coincident with IMPROVE's 1-in-3 day regimen. We
555   obtained quality-controlled samples from June-August 2014. Temporal variation in daily
556   values is consistent with IMPROVE for sulfate (r^2 = 0.86, slope = 1.03) and total mass (r^2 =
557   0.76, slope = 1.12). Differences between IMPROVE and SPARTAN are small for ASO_4
558   (36% vs. 30%), ANO_3 (2.4% vs. 1.1%), CM (11% vs. 7%), and EBC (4% vs. 3%). The

Atmospheric
Chemistry
and Physics
Discussions

Open Access

559   combined OM + unknown + water fraction IMPROVE was 51%, similar to the SPARTAN
560   RM mass fraction of 47%.
561
562   ### *4.12.8 Rehovot, Israel (n = 19)*
563   Rehovot is located on a four-story rooftop on the Weizmann Institute campus, 11 km from
564   the Mediterranean Sea and 20 km south of Tel Aviv. The city is surrounded by semi-arid, mixed-
565   use cropland, and the region experiences occasional Saharan desert dust outbreaks. Typical $PM_{2.5}$
566   concentrations are low (15 µg m^{-3}), with the composition in Rehovot consisting of 32% ASO_4,
567   18% RM and 13% CM. The RM fraction is smaller in Rehovot than at other SPARTAN sites
568   (22% total mass). Aerosol sources in Israel include agriculture, desert dust, traffic and coal-based
569   power plants (Graham et al., 2004). Relative sodium concentrations are significant in Rehovot
570   (6%), similar to Buenos Aires and Ilorin, and may include a contribution from dust. A spike in
571   ASO_4 concentrations occurred during the Lag Ba'Omer festival (May 7-18, 2015), during which
572   a large number of bonfires were lit nearby. During the festival, over 75% of total aerosol mass
573   came from $ASO_4 + ANO_3$, leading to a brief doubling of the hygroscopic parameter κ_v. We
574   observed a K:Al ratio of 38 for May 6th of the festival, the highest for any single filter.
575
576   *Saharan dust storm:* We had the opportunity to measure a severe dust storm in Rehovot from a
577   filter sampled February 4-13, 2015. The coarse filter Zn:Al ratio dropped to 0.02 during the
578   Saharan dust storm from the typical value of 0.3. On the coarse filter we obtained an absolute
579   CM mass of 950 µg, which accounts for half of the collected mass during the storm. 13% of dust
580   storm PM_c is combined sea salt, ANO_3, and ASO_4, leaving 35% RM. Although this RM fraction
581   may imply an incomplete mass reconstruction, it is possible that a significant portion of desert
582   dust consists of organic material (Falkovich et al., 2004).
583
584   ### *4.12.9 Atlanta, US (n = 13)*
585   Atlanta represents a major urban area in a developed country. The temporary SPARTAN site
586   was located at the South Dekalb supersite 15 km east of downtown Atlanta. Air sampling was
587   performed for a 4-month period spanning winter to spring 2014. Over the past 10 years
588   significant decreases in $PM_{2.5}$ have been observed here and across the eastern United States
589   (Boys et al., 2014). The surrounding region is tree-covered or agricultural.
590
591   *Atlanta* (*South Dekalb*) *Collocation:* Multi-year averaged data from the Chemical Speciation
592   Network (CSN) Atlanta station (USEPA, 2015) provides recent data from 2007-2013 for
593   comparison with 2014 SPARTAN data. The EPA OM fraction (60%) agrees well with the
594   SPARTAN mean RM (49%). Crustal, ANO_3, EBC and ASO_4 are within 4% relative to total
595   composition. Aerosol component fractions in Atlanta are consistent with Butler et al. (2003).
596   Other components CM (10%), ASO_4 (21%), and ANO_3 (3%) closely match their values,
597   except for EBC (11% vs. 3%).
598
599   ### *4.12.11 Hanoi, Vietnam (n = 10)*
600   Hanoi is an inland megacity surrounded by grassland and agriculture. The sampler itself is on
601   a building rooftop at the Vietnam Academy of Science, 5 km northwest of the city center.
602   Motorbikes are the main forms of transportation downtown and the primary source of mobile-
603   based $PM_{2.5}$ (Vu Van et al., 2013). In Hanoi the $PM_{2.5}$ Zn:Al ratio was 2.6, indicative of

Atmospheric
Chemistry
and Physics
Discussions

604 significant traffic and tire wear, is also the highest of any SPARTAN site. Biomass burning, coal
605 power, and cement are significant sources of $PM_{2.5}$ (Cohen et al., 2010).
606
607 *Hanoi Comparison:* SPARTAN differed with Cohen et al.(2010) regarding the contributions
608 of several compounds, perhaps related to differences in sampling season and location.
609 SPARTAN sea salt fraction was larger (2.5% vs. 0.6%), whereas ASO_4 (17%) was less than
610 reported by Cohen et al. (29%). Sulfate tends to be lower in the spring-summer seasons
611 (Cohen et al., 2010), coinciding with our measurement period, which may explain the
612 discrepancy. SPARTAN BC (9%) is close to Cohen et al. (2010), whereas SPARTAN RM
613 (49%) and CM (17%) masses are slightly larger.
614
615   ***4.12.12 Singapore, Singapore (n = 6)***
616   Singapore is a densely populated coastal city-state at 7,770 people/km^2. The sampler is
617 located on a rooftop at the National University of Singapore (NUS), near the center of the city.
618 Transportation is mixed-use, including taxis, rail, and bicycles, which may help explain the
619 relatively low EBC and CM of 3%. Despite this, the Zn:Al ratio remains high at 1.6, implying a
620 dominant traffic-based contribution to CM. SPARTAN instruments have observed significant
621 biomass burning downwind from Indonesia, causing an increase in absolute $PM_{2.5}$ from 32 in
622 August to 120 $\mu g\ m^{-3}$ in September 2015, as well as an increase in RM from 44% to 62%. The
623 K:Al ratio steadily increased during this same period, from 7.2 (Jul 24 – Aug 2, 2015) to 17 – 24
624 (Aug 11 – Sept 25).
625
626   ***4.12.12 Pretoria, South Africa (n = 5)***
627   Pretoria is a high-altitude city (1300 m) surrounded by arid, low-intensity agriculture and
628 extensive grasslands. The SPARTAN sampler is located on a 10m CSIR building rooftop 12 km
629 east of downtown area (*pop.* 700,000). Preliminary measurements of south-hemisphere
630 springtime show absolute $PM_{2.5}$ concentrations to be low, at 6.4 $\mu g\ m^{-3}$. There are significant
631 fractions of CM (22%) and EBC (22%), and low RM (14%). The Zn:Al ratio (0.69) indicates
632 vehicle traffic contributes to CM.

633 ## 5. Refining estimates of dry hourly $PM_{2.5}$ using κ_v

634 Our assessment of $PM_{2.5}$ hygroscopicity is determined by site-specific chemical composition. We
635 then use the time-varying hygroscopicity to refine the $PM_{2.5}$ values inferred from nephelometer
636 scatter.

637   ### 5.1. Relating $PM_{2.5}$ composition to κ_v

638   The outer pie charts of Figure 1 show the site-mean hygroscopic growth constant κ_v,
639 surrounded by the water contributions at 35% RH. The major contributors to PBW are ASO_4,
640 ANO_3, RM, and sea salt, as inferred from the values listed in Table 1 and weighted by
641 composition as in Eq. 5. ASO_4 and RM contribute similarly to total aerosol water whereas ANO_3
642 contributes less to $PM_{2.5}$ hygroscopicity due to its smaller mass. The contribution of sea salt to
643 hygroscopicity can be significant, and makes a dominant contribution in both Rehovot and
644 Buenos Aires.
645
646   The parameter κ_v, when averaged across all sites, is 0.19, similar to the generic estimate
647 $\kappa_{v,tot} = 0.2$ applied in the initial SPARTAN study (Snider et al., 2015). It is slightly larger than

Atmospheric
Chemistry
and Physics
Discussions

648   the value estimated (0.16 ± 0.07) by Padró et al. (2012) in Atlanta, GA. Liu et al. (2011) found
649   that κ_v varies between 0.25 and 0.34 in Northern China, for 50-250 nm sized particles. We found
650   significant long-term differences in $\kappa_{v,tot}$ between cities, from 0.14 in Dhaka to 0.32 in Rehovot,
651   and between filters at single sites (σ ~ 0.05). We found a slight tendency for $\kappa_{v,tot}$ to decrease
652   with average mass (r^2 = 0.06); however, temporal changes in mass were not strongly correlated
653   with $\kappa_{v,tot}$ ($r^2 < 0.01$). There are significant changes in $\kappa_{v,tot}$ due to seasonality and specific
654   events (e.g. dust storms, fires). In Beijing, aerosol hygroscopicity was 50% higher in mid
655   summer (August) due to increased sulfate, and in late winter (March) due to a relative increase in
656   sea salt. A summertime sulfate peak also agrees with observations by Yang et al. (2011).
657   Table 3 shows the site-specific PBW in PM$_{2.5}$. At RH =35%, PBW ranges from 1 − 6 μg m^{-3},
658   comparable to EBC. Above 80% RH, PBW will account for more than half of aerosol mass.
659   Accounting for this water component in nephelometer scatter motivates the following section.

660   ### 5.2. Relating nephelometer scatter to dry (RH=35%) PM$_{2.5}$

661   We apply a temporally resolved, site-specific κ_v to refine our relationship between total
662   nephelometer scatter and PM$_{2.5}$. We calculate a 45-day running mean aerosol volume-weighted
663   κ_v at each SPARTAN site. We then use the hygroscopic growth factors to estimate dry hourly
664   PM$_{2.5}$ from hourly nephelometer measurements of ambient scatter and hourly measured RH.
665   Appendix A2 describes the procedure in more detail.
666
667   We compared our hourly PM$_{2.5}$ in Beijing with PM$_{2.5}$ measurements from a Beta Attenuation
668   Monitor (MetOne) at the US Embassy, located 15 km away. The left panel of Figure 4 shows the
669   time series of hourly dry PM$_{2.5}$ concentrations predicted by SPARTAN during the summer.
670   Pronounced temporal variation is apparent, with PM$_{2.5}$ concentrations varying by more than an
671   order of magnitude. A high degree of consistency is found with the BAM (r^2 = 0.67). The
672   exclusion of water uptake in hourly PM$_{2.5}$ estimates (by setting all κ_v = 0) decreased hourly
673   correlations slightly to r^2 = 0.62. The average humidity in Beijing was just 47% for the
674   measurement period, corresponding to a mean 17% volume contribution by water (κ_v = 0.19),
675   which approaches our measurement error (Appendix A2). Hygroscopic compensation should
676   play a more significant role under more humid conditions (e.g. Manila and Dhaka).
677
678   The right panel shows daily-averaged PM$_{2.5}$ (n = 148). In 2014 there were 3167
679   coincidentally available hours with which to compare. The coefficient of variation for averaged
680   24-hour measurements remained high (r^2 = 0.71). There was a mean offset of 10 μg m^{-3}.
681   However the slope is near unity (0.98), suggesting excellent proportionality between our
682   nephelometer and the BAM instrument for PM$_{2.5}$ concentrations below 200 μg m^{-3}. Above this
683   concentration, nephelometer signals become non-linear. The agreement remained similar for
684   hourly values (r^2 = 0.67).
685

686   ## 6. Conclusions
687
688   We have established a multi-country network where continuous monitoring with a 3-
689   wavelength nephelometer is combined with a single multi-day composite filter sample to provide
690   information on PM$_{2.5}$. Long-term average aerosol composition is inferred from the filters,
691   including black carbon, sea salt, crustal material, ammonium sulfate, and ammonium nitrate.

Atmospheric
Chemistry
and Physics
Discussions

692 This composition information was applied to calculate aerosol hygroscopicity, and in turn the
693 relation between aerosol scatter at ambient and controlled RH. These data provide a consistent
694 set of compositional measurements from 12 sites in 11 countries.
695
696 We report ongoing measurements of fine particulate matter ($PM_{2.5}$), including compositional
697 information, in 12 locations over a three-year span (2013-2015). The mean composition averaged
698 for all SPARTAN sites is 20% ammonium sulfate, 12% crustal material, 11% equivalent black
699 carbon, 4% ammonium nitrate, 7% particle bound water (at 35% RH), 2% sea salt, 1% trace
700 element oxides, and 43% residual matter.
701
702 Analysis of filter samples reveals that several $PM_{2.5}$ chemical components varied by more
703 than an order of magnitude between sites. Ammonium sulfate ranged from 1 µg m^{-3} in Buenos
704 Aires to 17 µg m^{-3} in Kanpur (dry season). Ammonium nitrate ranged from 0.2 µg m^{-3}
705 (Mammoth Cave, summertime) to 6.7 µg m^{-3} (Kanpur, dry season). Equivalent black carbon
706 ranged from 0.7 µg m^{-3} (Mammoth Cave) to 8 µg m^{-3} (Dhaka, Bangladesh and Kanpur).
707
708 Crustal material concentrations ranged from 1 µg m^{-3} (Atlanta) to 13 µg m^{-3} (Beijing).
709 Measuring Zn:Al ratios in $PM_{2.5}$ was an effective way to determine anthropogenic contribution
710 to crustal material. Ratios larger than 0.5 identified sites with significant road dust contributions
711 (e.g. in Hanoi, Dhaka, Manila, and Kanpur). Some locations, such as Beijing and Buenos Aires,
712 had both high anthropogenic and natural crustal material. Low coarse Zn:Al ratios were apparent
713 during natural dust storms. Anthropogenic crustal material is an aerosol component neglected by
714 most global models and which may deserve more attention.
715
716 Potassium is a known marker for wood smoke; enhanced K:Al ratios were found in
717 Singapore downwind of Indonesian forest fires, in Kanpur during the winter dry season from
718 agricultural burning, and in Rehovot during a bonfire festival.
719
720 SPARTAN measurements generally agree well with previous collocated studies. SPARTAN
721 sulfate fractions are within 4% of fractions measured at eight of the ten collocated, though
722 temporally non-coincident, studies. Dedicated contemporaneous collocation with IMPROVE at
723 Mammoth Cave yielded a high degree of consistency with daily sulfate ($r^2 = 0.86$, slope = 1.03),
724 daily $PM_{2.5}$ ($r^2 = 0.76$, slope = 1.12), and mean fractions for all major $PM_{2.5}$ components (within
725 2%). Crustal material is typically consistent with the previous measurements, at 5-15%
726 composition. SPARTAN equivalent black carbon ranged broadly, from 3% (Singapore) to 25%
727 (Manila), and matched within a few percent of most previous works. Ammonium nitrate (4%)
728 generally matched other sites, though it was sometimes lower, as in Beijing and Atlanta. Sea-salt
729 was consistently less than 3% total mass, as found in previous measurements. Sea salt fractions
730 were highest in Buenos Aires and Rehovot (6%), reflecting natural coastal aerosols. SPARTAN
731 residual matter is consistent with the combined organic and unknown masses. Comparing with
732 collocated measurements supports the expectation that most of the RM is partially organic.
733 Residual matter could also include unaccounted-for particle bound water, measurement error,
734 and possibly unmeasured inorganic materials.
735
736 Seasonal tendencies are beginning to emerge within the SPARTAN study. Ammonium
737 sulfate concentrations remained relatively stable at 10-30% and reflect a variety of regional

Atmospheric
Chemistry
and Physics
Discussions

738 combustion sources. In Kanpur, Beijing, and Dhaka, ammonium nitrate reached peak relative
739 concentrations (> 7 %) during wintertime, due to lower temperatures. By contrast, summertime
740 ammonium nitrate in Mammoth Cave was much lower, at 1.5%. Ammonium sulfate and residual
741 matter concentrations increase in tandem, which implies related sources. We also observed
742 relatively high crustal material mass fractions in Bandung during two months of 2014 volcanic
743 activity, and in the springtime for Beijing during regional dust episodes. Subsequent work will
744 explore temporal variation in detail.

746 We calculated the hygroscopic constant κ_v for individual $PM_{2.5}$ filters to estimate water at
747 variable humidity, and to infer wet and water-free residual matter. Based on a range of literature,
748 we treated residual matter as mostly organic, with constant $\kappa_{v,RM} = 0.1$. Residual matter and
749 ammonium sulfate contributed the most to overall water uptake in aerosols. These individual
750 species, along with sea salt and ammonium nitrate, resulted in a mean mixed hygroscopic
751 constant of 0.19, implying that for many sites, water content above 80% RH will account for
752 more than half of aerosol mass. For cleanroom conditions of low humidity (35% RH), mean
753 water composition was estimated to be 7% by mass.

755 Water retention calculations allow for volumetric fluctuations estimates of aerosol water
756 at variable RH. We subtracted the water component to predict dry nephelometer scatter as a
757 function of time, anchored to filter masses at 35% RH. For Beijing, we assessed the consistency
758 of SPARTAN predictions of hourly $PM_{2.5}$ values with BAM measurements taken 15km away,
759 and found temporal consistency ($r^2 = 0.67$), with a slope near unity (0.98). The explained
760 variance decreased to $r^2 = 0.62$ when setting $\kappa_v = 0$. This comparison tested both SPARTAN
761 instrumentation and our treatment of aerosol water uptake.

763 These measurements provide chemical and physical data for future health research on
764 $PM_{2.5}$. Collocation with sun photometer measurements of AOD connects satellites observations
765 to ground-based measurements and provides information needed to evaluate chemical transport
766 model simulations of the $PM_{2.5}$ to AOD ratio. As sampling expands, SPARTAN will provide
767 long-term data on fine aerosol variability from around the world. Future work includes an
768 analysis of trace metal concentrations (Snider et al., in prep.) and applying SPARTAN
769 measurements to evaluate the $PM_{2.5}$ to AOD ratio in a chemical transport model (Weagle et al.,
770 in prep.). The data are freely available as a public good at www.spartan-network.org. We
771 welcome expressions of interest to join this grass-roots network.

Atmospheric
Chemistry
and Physics

Discussions

Open Access

EGU

7. References

787
788   Ahmed, S.: Food and Agriculture in Bangladesh, Encycl. Food Agric. Ethics, doi:10.1007/978-94-007-6167-4_61-2,
789   2013.

790   Asa-Awuku, A., Moore, R. H., Nenes, A., Bahreini, R., Holloway, J. S., Brock, C. A., Middlebrook, A. M.,
791   Ryerson, T. B., Jimenez, J. L., DeCarlo, P. F., Hecobian, A., Weber, R. J., Stickel, R., Tanner, D. J., and Huey, L.
792   G.: Airborne cloud condensation nuclei measurements during the 2006 Texas Air Quality Study, J. Geophys. Res.
793   Atmos., 116(D11), D11201, doi:10.1029/2010JD014874, 2011.

794   Badger, C. L., George, I., Griffiths, P. T., Braban, C. F., Cox, R. A., and Abbatt, J. P. D.: Phase transitions and
795   hygroscopic growth of aerosol particles containing humic acid and mixtures of humic acid and ammonium sulphate,
796   Atmos. Chem. Phys., 6(3), 755–768, doi:10.5194/acp-6-755-2006, 2006.

797   Barnard, J. C., Volkamer, R., and Kassianov, E. I.: Estimation of the mass absorption cross section of the organic
798   carbon component of aerosols in the Mexico City Metropolitan Area, Atmos. Chem. Phys., 8(22), 6665–6679,
799   doi:10.5194/acp-8-6665-2008, 2008.

800   Begum, B. A., Biswas, S. K., Markwitz, A., and Hopke, P. K.: Identification of sources of fine and coarse particulate
801   matter in Dhaka, Bangladesh, Aerosol Air Qual. Res., 10, 345–353, doi:10.4209/aaqr.2009.12.0082, 2010.

802   Begum, B. A., Hossain, A., Nahar, N., Markwitz, A., and Hopke, P. K.: Organic and Black Carbon in PM2.5 at an
803   Urban Site at Dhaka, Bangladesh, Aerosol Air Qual. Res., 12(6), 1062–1072, 2012.

804   Behera, S. N. and Sharma, M.: Reconstructing Primary and Secondary Components of PM2.5 Composition for an
805   Urban Atmosphere, Aerosol Sci. Technol., 44(11), 983–992, doi:10.1080/02786826.2010.504245, 2010.

806   Bell, M. L., Dominici, F., Ebisu, K., Zeger, S. L., and Samet, J. M.: Spatial and Temporal Variation in PM2.5
807   Chemical Composition in the United States for Health Effects Studies, Environ. Health Perspect., 115(7), 989–995,
808   doi:10.2307/4619499, 2007.

809   Bezantakos, S., Barmpounis, K., Giamarelou, M., Bossioli, E., Tombrou, M., Mihalopoulos, N., Eleftheriadis, K.,
810   Kalogiros, J., D. Allan, J., Bacak, A., Percival, C. J., Coe, H., and Biskos, G.: Chemical composition and
811   hygroscopic properties of aerosol particles over the Aegean Sea, Atmos. Chem. Phys., 13(22), 11595–11608,
812   doi:10.5194/acp-13-11595-2013, 2013.

813   Bond, T. C. and Bergstrom, R. W.: Light Absorption by Carbonaceous Particles: An Investigative Review, Aerosol
814   Sci. Technol., 40(1), 27–67, doi:10.1080/02786820500421521, 2006.

815   Boys, B. L., Martin, R. V, van Donkelaar, A., MacDonell, R. J., Hsu, N. C., Cooper, M. J., Yantosca, R. M., Lu, Z.,
816   Streets, D. G., Zhang, Q., and Wang, S. W.: Fifteen-Year Global Time Series of Satellite-Derived Fine Particulate
817   Matter, Environ. Sci. Technol., 48(19), 11109–11118, doi:10.1021/es502113p, 2014.

818   Brauer, M., Freedman, G., Frostad, J., van Donkelaar, A., Martin, R. V, Dentener, F., Dingenen, R. van, Estep, K.,
819   Amini, H., Apte, J. S., Balakrishnan, K., Barregard, L., Broday, D., Feigin, V., Ghosh, S., Hopke, P. K., Knibbs, L.
820   D., Kokubo, Y., Liu, Y., Ma, S., Morawska, L., Sangrador, J. L. T., Shaddick, G., Anderson, H. R., Vos, T.,
821   Forouzanfar, M. H., Burnett, R. T., and Cohen, A.: Ambient Air Pollution Exposure Estimation for the Global
822   Burden of Disease 2013, Environ. Sci. Technol., doi:10.1021/acs.est.5b03709, 2015.

823   Butler, A. J., Andrew, M. S., and Russell, A. G.: Daily sampling of PM2.5 in Atlanta: Results of the first year of the
824   Assessment of Spatial Aerosol Composition in Atlanta study, J. Geophys. Res. Atmos., 108(D7), 8415,
825   doi:10.1029/2002JD002234, 2003.

826   Canagaratna, M. R., Jimenez, J. L., Kroll, J. H., Chen, Q., Kessler, S. H., Massoli, P., Hildebrandt Ruiz, L., Fortner,
827   E., Williams, L. R., Wilson, K. R., Surratt, J. D., Donahue, N. M., Jayne, J. T., and Worsnop, D. R.: Elemental ratio
828   measurements of organic compounds using aerosol mass spectrometry: characterization, improved calibration, and

829 implications, Atmos. Chem. Phys., 15(1), 253–272, doi:10.5194/acp-15-253-2015, 2015.

830 Carrico, C. M., Petters, M. D., Kreidenweis, S. M., Sullivan, A. P., McMeeking, G. R., Levin, E. J. T., Engling, G.,
831 Malm, W. C., and Collett, J. L.: Water uptake and chemical composition of fresh aerosols generated in open burning
832 of biomass, Atmos. Chem. Phys., 10(11), 5165–5178, doi:10.5194/acp-10-5165-2010, 2010.

833 Chakraborty, A., Bhattu, D., Gupta, T., Tripathi, S. N., and Canagaratna, M. R.: Real-time measurements of ambient
834 aerosols in a polluted Indian city: Sources, characteristics, and processing of organic aerosols during foggy and
835 nonfoggy periods, J. Geophys. Res. Atmos., 120(17), 2015JD023419, doi:10.1002/2015JD023419, 2015.

836 Chang, R. Y.-W., Slowik, J. G., Shantz, N. C., Vlasenko, A., Liggio, J., Sjostedt, S. J., Leaitch, W. R., and Abbatt, J.
837 P. D.: The hygroscopicity parameter (κ) of ambient organic aerosol at a field site subject to biogenic and
838 anthropogenic influences: relationship to degree of aerosol oxidation, Atmos. Chem. Phys., 10(11), 5047–5064,
839 doi:10.5194/acp-10-5047-2010, 2010.

840 Chen, H., Goldberg, M. S., and Villeneuve, P. J.: A systematic review of the relation between long-term exposure to
841 ambient air pollution and chronic diseases., Rev. Environ. Health, 23(4), 243–297, 2008.

842 Chen, Z., Wang, J.-N., Ma, G.-X., and Zhang, Y.-S.: China tackles the health effects of air pollution, Lancet,
843 382(9909), 1959–1960, 2013.

844 Chow, J. C., Watson, J. G., Park, K., Lowenthal, D. H., Robinson, N. F., and Magliano, K. A.: Comparison of
845 particle light scattering and fine particulate matter mass in central California., J. Air Waste Manage. Assoc., 56(4),
846 398–410, 2006.

847 Chu, S.-H.: PM2.5 episodes as observed in the speciation trends network, Atmos. Environ., 38(31), 5237–5246,
848 doi:10.1016/j.atmosenv.2004.01.055, 2004.

849 Clarisse, L., Clerbaux, C., Dentener, F., Hurtmans, D., and Coheur, P.-F.: Global ammonia distribution derived from
850 infrared satellite observations, Nat. Geosci, 2(7), 479–483, 2009.

851 Cohen, D. D., Garton, D., Stelcer, E., Wang, T., Poon, S., Kim, J., Oh, S. N., Shin, H.-J., Ko, M. Y., and Santos, F.:
852 Characterisation of PM2. 5 and PM10 fine particle pollution in several Asian regions., 2002.

853 Cohen, D. D., Stelcer, E., Santos, F. L., Prior, M., Thompson, C., and Pabroa, P. C. B.: Fingerprinting and source
854 apportionment of fine particle pollution in Manila by IBA and PMF techniques: A 7-year study, X-Ray Spectrom.,
855 38(1), 18–25, doi:10.1002/xrs.1112, 2009.

856 Cohen, D. D., Crawford, J., Stelcer, E., and Bac, V. T.: Characterisation and source apportionment of fine
857 particulate sources at Hanoi from 2001 to 2008, Atmos. Environ., 44(3), 320–328,
858 doi:10.1016/j.atmosenv.2009.10.037, 2010.

859 Councell, T. B., Duckenfield, K. U., Landa, E. R., and Callender, E.: Tire-Wear Particles as a Source of Zinc to the
860 Environment, Environ. Sci. Technol., 38(15), 4206–4214, doi:10.1021/es034631f, 2004.

861 Dabek-Zlotorzynska, E., Dann, T. F., Kalyani Martinelango, P., Celo, V., Brook, J. R., Mathieu, D., Ding, L., and
862 Austin, C. C.: Canadian National Air Pollution Surveillance (NAPS) PM2.5 speciation program: Methodology and
863 PM2.5 chemical composition for the years 2003–2008, Atmos. Environ., 45(3), 673–686, 2011.

864 Duplissy, J., DeCarlo, P. F., Dommen, J., Alfarra, M. R., Metzger, A., Barmpadimos, I., Prevot, A. S. H.,
865 Weingartner, E., Tritscher, T., Gysel, M., Aiken, A. C., Jimenez, J. L., Canagaratna, M. R., Worsnop, D. R., Collins,
866 D. R., Tomlinson, J., and Baltensperger, U.: Relating hygroscopicity and composition of organic aerosol particulate
867 matter, Atmos. Chem. Phys., 11(3), 1155–1165, doi:10.5194/acp-11-1155-2011, 2011.

868 Dusek, U., Frank, G. P., Massling, A., Zeromskiene, K., Iinuma, Y., Schmid, O., Helas, G., Hennig, T.,
869 Wiedensohler, A., and Andreae, M. O.: Water uptake by biomass burning aerosol at sub- and supersaturated
870 conditions: closure studies and implications for the role of organics, Atmos. Chem. Phys., 11(18), 9519–9532,
871 doi:10.5194/acp-11-9519-2011, 2011.

872 Falkovich, A. H., Schkolnik, G., Ganor, E., and Rudich, Y.: Adsorption of organic compounds pertinent to urban
873 environments onto mineral dust particles, J. Geophys. Res. Atmos., 109(D2), n/a–n/a, doi:10.1029/2003JD003919,
874 2004.

Atmospheric
Chemistry
and Physics
Discussions

Open Access

EGU

875 Fang, T., Guo, H., Verma, V., Peltier, R. E., and Weber, R. J.: $PM_{2.5}$ water-soluble elements in the southeastern
876 United States: automated analytical method development, spatiotemporal distributions, source apportionment, and
877 implications for heath studies, Atmos. Chem. Phys., 15(20), 11667–11682, doi:10.5194/acp-15-11667-2015, 2015.

878 Forouzanfar, M. H., Alexander, L., Anderson, H. R., Bachman, V. F., Biryukov, S., Brauer, M., Burnett, R., Casey,
879 D., Coates, M. M., Cohen, A., Delwiche, K., Estep, K., Frostad, J. J., KC, A., Kyu, H. H., Moradi-Lakeh, M., Ng,
880 M., Slepak, E. L., Thomas, B. A., Wagner, J., Aasvang, G. M., Abbafati, C., Ozgoren, A. A., Abd-Allah, F., Abera,
881 S. F., Aboyans, V., Abraham, B., Abraham, J. P., Abubakar, I., Abu-Rmeileh, N. M. E., Aburto, T. C., Achoki, T.,
882 Adelekan, A., Adofo, K., Adou, A. K., Adsuar, J. C., Afshin, A., Agardh, E. E., Al Khabouri, M. J., Al Lami, F. H.,
883 Alam, S. S., Alasfoor, D., Albittar, M. I., Alegretti, M. A., Aleman, A. V, Alemu, Z. A., Alfonso-Cristancho, R.,
884 Alhabib, S., Ali, R., Ali, M. K., Alla, F., Allebeck, P., Allen, P. J., Alsharif, U., Alvarez, E., Alvis-Guzman, N.,
885 Amankwaa, A. A., Amare, A. T., Ameh, E. A., Ameli, O., Amini, H., Ammar, W., Anderson, B. O., Antonio, C. A.
886 T., Anwari, P., Cunningham, S. A., Arnlöv, J., Arsenijevic, V. S. A., Artaman, A., Asghar, R. J., Assadi, R., Atkins,
887 L. S., Atkinson, C., Avila, M. A., Awuah, B., Badawi, A., Bahit, M. C., Bakfalouni, T., Balakrishnan, K., Balalla,
888 S., Balu, R. K., Banerjee, A., Barber, R. M., Barker-Collo, S. L., Barquera, S., Barregard, L., Barrero, L. H.,
889 Barrientos-Gutierrez, T., Basto-Abreu, A. C., Basu, A., Basu, S., Basulaiman, M. O., Ruvalcaba, C. B., Beardsley,
890 J., Bedi, N., Bekele, T., Bell, M. L., Benjet, C., Bennett, D. A., et al.: Global, regional, and national comparative risk
891 assessment of 79 behavioural, environmental and occupational, and metabolic risks or clusters of risks in 188
892 countries, 1990–2013: a systematic analysis for the Global Burden of Disease Study 2013, Lancet,
893 doi:10.1016/S0140-6736(15)00128-2, 2015.

894 Fountoukis, C. and Nenes, A.: ISORROPIA II: a computationally efficient thermodynamic equilibrium model for
895 aerosols, Atmos. Chem. Phys., 7(17), 4639–4659, doi:10.5194/acp-7-4639-2007, 2007.

896 Fujii, Y., Iriana, W., Oda, M., Puriwigati, A., Tohno, S., Lestari, P., Mizohata, A., and Huboyo, H. S.:
897 Characteristics of carbonaceous aerosols emitted from peatland fire in Riau, Sumatra, Indonesia, Atmos. Environ.,
898 87, 164–169, doi:10.1016/j.atmosenv.2014.01.037, 2014.

899 Generoso, S., Bréon, F.-M., Balkanski, Y., Boucher, O., and Schulz, M.: Improving the seasonal cycle and
900 interannual variations of biomass burning aerosol sources, Atmos. Chem. Phys., 3(4), 1211–1222, doi:10.5194/acp-
901 3-1211-2003, 2003.

902 Gibson, M. D., Heal, M. R., Bache, D. H., Hursthouse, A. S., Beverland, I. J., Craig, S. E., Clark, C. F., Jackson, M.
903 H., Guernsey, J. R., and Jones, C.: Using Mass Reconstruction along a Four-Site Transect as a Method to Interpret
904 PM10 in West-Central Scotland,United Kingdom, J. Air Waste Manage. Assoc., 59(12), 1429–1436,
905 doi:10.3155/1047-3289.59.12.1429, 2009.

906 Gibson, M. D., Pierce, J. R., Waugh, D., Kuchta, J. S., Chisholm, L., Duck, T. J., Hopper, J. T., Beauchamp, S.,
907 King, G. H., Franklin, J. E., Leaitch, W. R., Wheeler, A. J., Li, Z., Gagnon, G. A., and Palmer, P. I.: Identifying the
908 sources driving observed PM2.5 temporal variability over Halifax, Nova Scotia, during BORTAS-B, Atmos. Chem.
909 Phys., 13(14), 7199–7213, doi:10.5194/acp-13-7199-2013, 2013a.

910 Gibson, M. D., Heal, M. R., Li, Z., Kuchta, J., King, G. H., Hayes, A., and Lambert, S.: The spatial and seasonal
911 variation of nitrogen dioxide and sulfur dioxide in Cape Breton Highlands National Park, Canada, and the
912 association with lichen abundance, Atmos. Environ., 64(0), 303–311,
913 doi:http://dx.doi.org/10.1016/j.atmosenv.2012.09.068, 2013b.

914 Giordano, M. R., Short, D. Z., Hosseini, S., Lichtenberg, W., and Asa-Awuku, A. A.: Changes in Droplet Surface
915 Tension Affect the Observed Hygroscopicity of Photochemically Aged Biomass Burning Aerosol, Environ. Sci.
916 Technol., 47(19), 10980–10986, doi:10.1021/es401867j, 2013.

917 Graham, B., Falkovich, A. H., Rudich, Y., Maenhaut, W., Guyon, P., and Andreae, M. O.: Local and regional
918 contributions to the atmospheric aerosol over Tel Aviv, Israel: a case study using elemental, ionic and organic
919 tracers, Atmos. Environ., 38(11), 1593–1604, doi:http://dx.doi.org/10.1016/j.atmosenv.2003.12.015, 2004.

920 Hand, J. and Malm, W. C.: Review of the IMPROVE Equation for Estimating Ambient Light Extinction
921 Coefficients, Colorado State University, Fort Colins., 2006.

922 Hand, J. L., Schichtel, B. A., Pitchford, M., Malm, W. C., and Frank, N. H.: Seasonal composition of remote and
923 urban fine particulate matter in the United States, J. Geophys. Res., 117(D5), D05209, doi:10.1029/2011JD017122,

Atmospheric
Chemistry
and Physics
Discussions

924   2012.

925   Henning, S., Weingartner, E., Schwikowski, M., Gäggeler, H. W., Gehrig, R., Hinz, K.-P., Trimborn, A., Spengler,
926   B., and Baltensperger, U.: Seasonal variation of water-soluble ions of the aerosol at the high-alpine site Jungfraujoch
927   (3580 m asl), J. Geophys. Res. Atmos., 108(D1), 4030, doi:10.1029/2002JD002439, 2003.

928   Hersey, S. P., Craven, J. S., Metcalf, A. R., Lin, J., Lathem, T., Suski, K. J., Cahill, J. F., Duong, H. T., Sorooshian,
929   A., Jonsson, H. H., Shiraiwa, M., Zuend, A., Nenes, A., Prather, K. A., Flagan, R. C., and Seinfeld, J. H.:
930   Composition and hygroscopicity of the Los Angeles Aerosol: CalNex, J. Geophys. Res. Atmos., 118(7), 3016–3036,
931   doi:10.1002/jgrd.50307, 2013.

932   Holben, B. N., Eck, T. F., Slutsker, I., Tanré, D., Buis, J. P., Setzer, A., Vermote, E., Reagan, J. A., Kaufman, Y. J.,
933   Nakajima, T., Lavenu, F., Jankowiak, I., and Smirnov, A.: AERONET—A Federated Instrument Network and Data
934   Archive for Aerosol Characterization, Remote Sens. Environ., 66(1), 1–16, doi:http://dx.doi.org/10.1016/S0034-
935   4257(98)00031-5, 1998.

936   Huang, J. P., Liu, J. J., Chen, B., and Nasiri, S. L.: Detection of anthropogenic dust using CALIPSO lidar
937   measurements, Atmos. Chem. Phys., 15(20), 11653–11665, doi:10.5194/acp-15-11653-2015, 2015.

938   IMPROVE: Reconstructing Light Extinction from Aerosol Measurements, Reconstr. Light Extinction from Aerosol
939   Meas. Interag. Monit. Prot. Vis. Environ. [online] Available from:
940   http://views.cira.colostate.edu/fed/DataWizard/Default.aspx (Accessed 20 May 2012), 2015.

941   IPCC: Climate Change 2013: The Physical Science Basis. Contribution of Working Group I to the Fifth Assessment
942   Report of the Intergovernmental Panel on Climate Change, 5th ed., edited by T. F. Stocker, D. Qin, G.-K. Plattner,
943   M. Tignor, S. K. Allen, J. Boschung, A. Nauels, Y. Xia, V. Bex, and P. M. Midgley, Cambridge University Press,
944   Cambridge, United Kingdom and New York, NY, USA., 2013.

945   Jasan, R. C., Plá, R. R., Invernizzi, R., and Dos Santos, M.: Characterization of atmospheric aerosol in Buenos
946   Aires, Argentina, J. Radioanal. Nucl. Chem., 281(1), 101–105, doi:10.1007/s10967-009-0071-1, 2009.

947   Jimenez, J. L., Canagaratna, M. R., Donahue, N. M., Prevot, A. S. H., Zhang, Q., Kroll, J. H., DeCarlo, P. F., Allan,
948   J. D., Coe, H., Ng, N. L., Aiken, A. C., Docherty, K. S., Ulbrich, I. M., Grieshop, A. P., Robinson, A. L., Duplissy,
949   J., Smith, J. D., Wilson, K. R., Lanz, V. A., Hueglin, C., Sun, Y. L., Tian, J., Laaksonen, A., Raatikainen, T.,
950   Rautiainen, J., Vaattovaara, P., Ehn, M., Kulmala, M., Tomlinson, J. M., Collins, D. R., Cubison, M. J., E., Dunlea,
951   J., Huffman, J. A., Onasch, T. B., Alfarra, M. R., Williams, P. I., Bower, K., Kondo, Y., Schneider, J., Drewnick, F.,
952   Borrmann, S., Weimer, S., Demerjian, K., Salcedo, D., Cottrell, L., Griffin, R., Takami, A., Miyoshi, T.,
953   Hatakeyama, S., Shimono, A., Sun, J. Y., Zhang, Y. M., Dzepina, K., Kimmel, J. R., Sueper, D., Jayne, J. T.,
954   Herndon, S. C., Trimborn, A. M., Williams, L. R., Wood, E. C., Middlebrook, A. M., Kolb, C. E., Baltensperger, U.,
955   and Worsnop, D. R.: Evolution of Organic Aerosols in the Atmosphere, Sci. , 326 (5959), 1525–1529,
956   doi:10.1126/science.1180353, 2009.

957   Kahn, R. A. and Gaitley, B. J.: An analysis of global aerosol type as retrieved by MISR, J. Geophys. Res. Atmos.,
958   120(9), 4248–4281, doi:10.1002/2015JD023322, 2015.

959   Kloog, I., Koutrakis, P., Coull, B. A., Lee, H. J., and Schwartz, J.: Assessing temporally and spatially resolved
960   PM2.5 exposures for epidemiological studies using satellite aerosol optical depth measurements, Atmos. Environ.,
961   45(35), 6267–6275, doi:10.1016/j.atmosenv.2011.08.066, 2011.

962   Kloog, I., Ridgway, B., Koutrakis, P., Coull, B. A., and Schwartz, J. D.: Long- and Short-Term Exposure to PM(2.5)
963   and Mortality: Using Novel Exposure Models, Epidemiology, 24(4), 555–561,
964   doi:10.1097/EDE.0b013e318294beaa, 2013.

965   Koepke, P., Hess, M., Schult, I., and Shettle, E. P.: Global Aerosol Dataset, Report N 243, Hamburg., 1997.

966   Kreidenweis, S. M., Petters, M. D., and DeMott, P. J.: Single-parameter estimates of aerosol water content, Environ.
967   Res. Lett., 3(3), 35002, doi:10.1088/1748-9326/3/3/035002, 2008.

968   Laden, F., Schwartz, J., Speizer, F. E., and Dockery, D. W.: Reduction in Fine Particulate Air Pollution and
969   Mortality, Am. J. Respir. Crit. Care Med., 173(6), 667–672, doi:10.1164/rccm.200503-443OC, 2006.

970   Latham, J., Cumani, R., Rosati, I., and Bloise, M.: Global Land Cover SHARE (GLC-SHARE) database Beta-

Atmospheric
Chemistry
and Physics
Discussions

971   Release Version 1.0-2014, Rome., 2014.

972   Lathem, T. L., Beyersdorf, A. J., Thornhill, K. L., Winstead, E. L., Cubison, M. J., Hecobian, A., Jimenez, J. L.,
973   Weber, R. J., Anderson, B. E., and Nenes, A.: Analysis of CCN activity of Arctic aerosol and Canadian biomass
974   burning during summer 2008, Atmos. Chem. Phys., 13(5), 2735–2756, doi:10.5194/acp-13-2735-2013, 2013.

975   Lee, H. J., Coull, B. A., Bell, M. L., and Koutrakis, P.: Use of satellite-based aerosol optical depth and spatial
976   clustering to predict ambient PM2.5 concentrations., Environ. Res., 118, 8–15, doi:10.1016/j.envres.2012.06.011,
977   2012.

978   Lelieveld, J., Evans, J. S., Fnais, M., Giannadaki, D., and Pozzer, A.: The contribution of outdoor air pollution
979   sources to premature mortality on a global scale, Nature, 525(7569), 367–371, 2015.

980   Lepeule, J., Laden, F., Dockery, D., and Schwartz, J.: Chronic Exposure to Fine Particles and Mortality: An
981   Extended Follow-up of the Harvard Six Cities Study from 1974 to 2009, Environ. Health Perspect., 120(7), 965–
982   970, doi:10.1289/ehp.1104660, 2012.

983   Lestari, P. and Mauliadi, Y. D.: Source apportionment of particulate matter at urban mixed site in Indonesia using
984   PMF, Atmos. Environ., 43(10), 1760–1770, doi:http://dx.doi.org/10.1016/j.atmosenv.2008.12.044, 2009.

985   Lin, C., Li, Y., Yuan, Z., Lau, A. K. H., Li, C., and Fung, J. C. H.: Using satellite remote sensing data to estimate the
986   high-resolution distribution of ground-level PM2.5, Remote Sens. Environ., 156, 117–128,
987   doi:10.1016/j.rse.2014.09.015, 2015.

988   Liu, P. F., Zhao, C. S., Göbel, T., Hallbauer, E., Nowak, A., Ran, L., Xu, W. Y., Deng, Z. Z., Ma, N., Mildenberger,
989   K., Henning, S., Stratmann, F., and Wiedensohler, A.: Hygroscopic properties of aerosol particles at high relative
990   humidity and their diurnal variations in the North China Plain, Atmos. Chem. Phys., 11(7), 3479–3494,
991   doi:10.5194/acp-11-3479-2011, 2011.

992   Liu, Y., Monod, A., Tritscher, T., Praplan, A. P., DeCarlo, P. F., Temime-Roussel, B., Quivet, E., Marchand, N.,
993   Dommen, J., and Baltensperger, U.: Aqueous phase processing of secondary organic aerosol from isoprene
994   photooxidation, Atmos. Chem. Phys., 12(13), 5879–5895, doi:10.5194/acp-12-5879-2012, 2012.

995   Malm, W. C., Sisler, J. F., Huffman, D., Eldred, R. A., and Cahill, T. A.: Spatial and seasonal trends in particle
996   concentration and optical extinction in the United States, J. Geophys. Res., 99(D1), 1347–1370, 1994.

997   Misra, A., Gaur, A., Bhattu, D., Ghosh, S., Dwivedi, A. K., Dalai, R., Paul, D., Gupta, T., Tare, V., Mishra, S. K.,
998   Singh, S., and Tripathi, S. N.: An overview of the physico-chemical characteristics of dust at Kanpur in the central
999   Indo-Gangetic basin, Atmos. Environ., 97, 386–396, doi:10.1016/j.atmosenv.2014.08.043, 2014.

1000   Munchak, L. A., Schichtel, B. A., Sullivan, A. P., Holden, A. S., Kreidenweis, S. M., Malm, W. C., and Collett, J.
1001   L.: Development of wildland fire particulate smoke marker to organic carbon emission ratios for the conterminous
1002   United States, Atmos. Environ., 45(2), 395–403, doi:10.1016/j.atmosenv.2010.10.006, 2011.

1003   Oanh, N. T. K., Upadhyay, N., Zhuang, Y.-H., Hao, Z.-P., Murthy, D. V. S., Lestari, P., Villarin, J. T., Chengchua,
1004   K., Co, H. X., Dung, N. T., and Lindgren, E. S.: Particulate air pollution in six Asian cities: Spatial and temporal
1005   distributions, and associated sources, Atmos. Environ., 40(18), 3367–3380,
1006   doi:http://dx.doi.org/10.1016/j.atmosenv.2006.01.050, 2006.

1007   Padró, L. T., Moore, R. H., Zhang, X., Rastogi, N., Weber, R. J., and Nenes, A.: Mixing state and compositional
1008   effects on CCN activity and droplet growth kinetics of size-resolved CCN in an urban environment, Atmos. Chem.
1009   Phys., 12(21), 10239–10255, doi:10.5194/acp-12-10239-2012, 2012.

1010   Patadia, F., Kahn, R. A., Limbacher, J. A., Burton, S. P., Ferrare, R. A., Hostetler, C. A., and Hair, J. W.: Aerosol
1011   airmass type mapping over the Urban Mexico City region from space-based multi-angle imaging, Atmos. Chem.
1012   Phys., 13(18), 9525–9541, doi:10.5194/acp-13-9525-2013, 2013.

1013   Petters, M. D. and Kreidenweis, S. M.: A single parameter representation of hygroscopic growth and cloud
1014   condensation nucleus activity, Atmos. Chem. Phys., 7(8), 1961–1971, doi:10.5194/acp-7-1961-2007, 2007.

1015   Petters, M. D. and Kreidenweis, S. M.: A single parameter representation of hygroscopic growth and cloud
1016   condensation nucleus activity – Part 2: Including solubility, Atmos. Chem. Phys., 8(20), 6273–6279,

1017   doi:10.5194/acp-8-6273-2008, 2008.

1018   Petters, M. D. and Kreidenweis, S. M.: A single parameter representation of hygroscopic growth and cloud
1019   condensation nucleus activity; Part 3: Including surfactant partitioning, Atmos. Chem. Phys., 13(2), 1081–1091,
1020   doi:10.5194/acp-13-1081-2013, 2013.

1021   Petzold, A., Ogren, J. A., Fiebig, M., Laj, P., Li, S.-M., Baltensperger, U., Holzer-Popp, T., Kinne, S., Pappalardo,
1022   G., Sugimoto, N., Wehrli, C., Wiedensohler, A., and Zhang, X.-Y.: Recommendations for reporting "black carbon"
1023   measurements, Atmos. Chem. Phys., 13(16), 8365–8379, doi:10.5194/acp-13-8365-2013, 2013.

1024   Philip, S., Martin, R. V, van Donkelaar, A., Lo, J. W.-H., Wang, Y., Chen, D., Zhang, L., Kasibhatla, P. S., Wang,
1025   S., Zhang, Q., Lu, Z., Streets, D. G., Bittman, S., and Macdonald, D. J.: Global Chemical Composition of Ambient
1026   Fine Particulate Matter for Exposure Assessment, Environ. Sci. Technol., 48(22), 13060–13068,
1027   doi:10.1021/es502965b, 2014a.

1028   Philip, S., Martin, R. V., Pierce, J. R., Jimenez, J. L., Zhang, Q., Canagaratna, M. R., Spracklen, D. V., Nowlan, C.
1029   R., Lamsal, L. N., Cooper, M. J., and Krotkov, N. A.: Spatially and seasonally resolved estimate of the ratio of
1030   organic mass to organic carbon, Atmos. Environ., 87, 34–40, doi:10.1016/j.atmosenv.2013.11.065, 2014b.

1031   Prenni, A. J., Petters, M. D., Kreidenweis, S. M., DeMott, P. J., and Ziemann, P. J.: Cloud droplet activation of
1032   secondary organic aerosol, J. Geophys. Res., 112(D10), D10223, doi:10.1029/2006JD007963, 2007.

1033   Putaud, J.-P., Raes, F., Van Dingenen, R., Brüggemann, E., Facchini, M.-C., Decesari, S., Fuzzi, S., Gehrig, R.,
1034   Hüglin, C., Laj, P., Lorbeer, G., Maenhaut, W., Mihalopoulos, N., Müller, K., Querol, X., Rodriguez, S., Schneider,
1035   J., Spindler, G., Brink, H. ten, Tørseth, K., and Wiedensohler, A.: A European aerosol phenomenology—2: chemical
1036   characteristics of particulate matter at kerbside, urban, rural and background sites in Europe, Atmos. Environ.,
1037   38(16), 2579–2595, doi:http://dx.doi.org/10.1016/j.atmosenv.2004.01.041, 2004.

1038   Putaud, J.-P., Van Dingenen, R., Alastuey, A., Bauer, H., Birmili, W., Cyrys, J., Flentje, H., Fuzzi, S., Gehrig, R.,
1039   Hansson, H. C., Harrison, R. M., Herrmann, H., Hitzenberger, R., Hüglin, C., Jones, A. M., Kasper-Giebl, A., Kiss,
1040   G., Kousa, A., Kuhlbusch, T. A. J., Löschau, G., Maenhaut, W., Molnar, A., Moreno, T., Pekkanen, J., Perrino, C.,
1041   Pitz, M., Puxbaum, H., Querol, X., Rodriguez, S., Salma, I., Schwarz, J., Smolik, J., Schneider, J., Spindler, G., ten
1042   Brink, H., Tursic, J., Viana, M., Wiedensohler, A., and Raes, F.: A European aerosol phenomenology – 3: Physical
1043   and chemical characteristics of particulate matter from 60 rural, urban, and kerbside sites across Europe, Atmos.
1044   Environ., 44(10), 1308–1320, doi:10.1016/j.atmosenv.2009.12.011, 2010.

1045   Quincey, P., Butterfield, D., Green, D., Coyle, M., and Cape, J. N.: An evaluation of measurement methods for
1046   organic, elemental and black carbon in ambient air monitoring sites, Atmos. Environ., 43(32), 5085–5091,
1047   doi:http://dx.doi.org/10.1016/j.atmosenv.2009.06.041, 2009.

1048   Ram, K., Sarin, M. M., and Tripathi, S. N.: Temporal Trends in Atmospheric PM2.5, PM10, Elemental Carbon,
1049   Organic Carbon, Water-Soluble Organic Carbon, and Optical Properties: Impact of Biomass Burning Emissions in
1050   The Indo-Gangetic Plain, Environ. Sci. Technol., 46(2), 686–695, doi:10.1021/es202857w, 2012.

1051   Remoundaki, E., Kassomenos, P., Mantas, E., Mihalopoulos, N., and Tsezos, M.: Composition and Mass Closure of
1052   PM2.5 in Urban Environment (Athens, Greece), Aerosol Air Qual. Res., 13(1), 72–82, 2013.

1053   Rickards, A. M. J., Miles, R. E. H., Davies, J. F., Marshall, F. H., and Reid, J. P.: Measurements of the Sensitivity of
1054   Aerosol Hygroscopicity and the κ Parameter to the O/C Ratio, J. Phys. Chem. A, 117(51), 14120–14131,
1055   doi:10.1021/jp407991n, 2013.

1056   Robinson, C. B., Schill, G. P., Zarzana, K. J., and Tolbert, M. A.: Impact of Organic Coating on Optical Growth of
1057   Ammonium Sulfate Particles, Environ. Sci. Technol., 47(23), 13339–13346, doi:10.1021/es4023128, 2013.

1058   Santoso, M., Dwiana Lestiani, D., and Hopke, P. K.: Atmospheric black carbon in PM2.5 in Indonesian cities, J. Air
1059   Waste Manage. Assoc., 63(9), 1022–1025, doi:10.1080/10962247.2013.804465, 2013.

1060   Snider, G., Weagle, C. L., Martin, R. V., van Donkelaar, A., Conrad, K., Cunningham, D., Gordon, C., Zwicker, M.,
1061   Akoshile, C., Artaxo, P., Anh, N. X., Brook, J., Dong, J., Garland, R. M., Greenwald, R., Griffith, D., He, K.,
1062   Holben, B. N., Kahn, R., Koren, I., Lagrosas, N., Lestari, P., Ma, Z., Vanderlei Martins, J., Quel, E. J., Rudich, Y.,
1063   Salam, A., Tripathi, S. N., Yu, C., Zhang, Q., Zhang, Y., Brauer, M., Cohen, A., Gibson, M. D., and Liu, Y.:

1064   SPARTAN: a global network to evaluate and enhance satellite-based estimates of ground-level particulate matter for
1065   global health applications, Atmos. Meas. Tech., 8(1), 505–521, doi:10.5194/amt-8-505-2015, 2015.

1066   Snider, G., et al.: Variation in Global Trace Metal components in PM2.5: Emerging Results from SPARTAN, in
1067   prep, 2016.

1068   Sorooshian, A., Hersey, S., Brechtel, F. J., Corless, A., Flagan, R. C., and Seinfeld, J. H.: Rapid, Size-Resolved
1069   Aerosol Hygroscopic Growth Measurements: Differential Aerosol Sizing and Hygroscopicity Spectrometer Probe
1070   (DASH-SP), Aerosol Sci. Technol., 42(6), 445–464, doi:10.1080/02786820802178506, 2008.

1071   Sun, Y.-L., Zhang, Q., Schwab, J. J., Demerjian, K. L., Chen, W.-N., Bae, M.-S., Hung, H.-M., Hogrefe, O., Frank,
1072   B., Rattigan, O. V., and Lin, Y.-C.: Characterization of the sources and processes of organic and inorganic aerosols
1073   in New York city with a high-resolution time-of-flight aerosol mass spectrometer, Atmos. Chem. Phys., 11(4),
1074   1581–1602, doi:10.5194/acp-11-1581-2011, 2011.

1075   Svenningsson, B., Rissler, J., Swietlicki, E., Mircea, M., Bilde, M., Facchini, M. C., Decesari, S., Fuzzi, S., Zhou, J.,
1076   Mønster, J., and Rosenørn, T.: Hygroscopic growth and critical supersaturations for mixed aerosol particles of
1077   inorganic and organic compounds of atmospheric relevance, Atmos. Chem. Phys., 6(7), 1937–1952,
1078   doi:10.5194/acp-6-1937-2006, 2006.

1079   Swietlicki, E., Hansson, H.-C., Hämeri, K., Svenningsson, B., Massling, A., McFiggans, G., McMurry, P. H., Petäjä,
1080   T., Tunved, P., Gysel, M., Topping, D., Weingartner, E., Baltensperger, U., Rissler, J., Wiedensohler, A., and
1081   Kulmala, M.: Hygroscopic properties of submicrometer atmospheric aerosol particles measured with H-TDMA
1082   instruments in various environments—a review, Tellus B, 60(3), 432–469, 2008.

1083   Taha, G., Box, G. P., Cohen, D. D., and Stelcer, E.: Black Carbon Measurement using Laser Integrating Plate
1084   Method, Aerosol Sci. Technol., 41(3), 266–276, doi:10.1080/02786820601156224, 2007.

1085   USEPA: Chemical Speciation Network Database, [online] Available from:
1086   http://views.cira.colostate.edu/fed/DataWizard/Default.aspx (Accessed 1 December 2015), 2015.

1087   van Donkelaar, A., Martin, R. V, Brauer, M., and Boys, B. L.: Use of Satellite Observations for Long-Term
1088   Exposure Assessment of Global Concentrations of Fine Particulate Matter, Environ. Health Perspect., 123(2), 135–
1089   143, doi:10.1289/ehp.1408646, 2015.

1090   Varutbangkul, V., Brechtel, F. J., Bahreini, R., Ng, N. L., Keywood, M. D., Kroll, J. H., Flagan, R. C., Seinfeld, J.
1091   H., Lee, A., and Goldstein, A. H.: Hygroscopicity of secondary organic aerosols formed by oxidation of
1092   cycloalkenes, monoterpenes, sesquiterpenes, and related compounds, Atmos. Chem. Phys., 6(9), 2367–2388,
1093   doi:10.5194/acp-6-2367-2006, 2006.

1094   Villalobos, A. M., Amonov, M. O., Shafer, M. M., Devi, J. J., Gupta, T., Tripathi, S. N., Rana, K. S., Mckenzie, M.,
1095   Bergin, M. H., and Schauer, J. J.: Source apportionment of carbonaceous fine particulate matter (PM2.5) in two
1096   contrasting cities across the Indo–Gangetic Plain, Atmos. Pollut. Res., 6(3), 398, 2015.

1097   Vu Van, H., Le Xuan, Q., Pham Ngoc, H., and Luc, H.: Health Risk Assessment of Mobility-Related Air Pollution
1098   in Ha Noi, Vietnam, J. Environ. Prot. (Irvine,. Calif.), 4(10), 1165–1172, 2013.

1099   Wagner, F., Bortoli, D., Pereira, S., João Costa, M., Silva, A. M., Weinzierl, B., Esselborn, M., Petzold, A., Rasp,
1100   K., Heinold, B., and Tegen, I.: Properties of dust aerosol particles transported to Portugal from the Sahara desert,
1101   Tellus B, 61(1), 297–306, 2009.

1102   Wang, J. L.: Mapping the Global Dust Storm Records: Review of Dust Data Sources in Supporting
1103   Modeling/Climate Study, Curr. Pollut. Reports, 1(2), 82–94, doi:10.1007/s40726-015-0008-y, 2015.

1104   Wang, Z., Chen, L., Tao, J., Zhang, Y., and Su, L.: Satellite-based estimation of regional particulate matter (PM) in
1105   Beijing using vertical-and-RH correcting method, Remote Sens. Environ., 114(1), 50–63,
1106   doi:http://dx.doi.org/10.1016/j.rse.2009.08.009, 2010.

1107   Weagle, C. L., et al.: Interpretation of measurements from SPARTAN to examine factors affecting spatial variation
1108   in the relationship between ground level fine particulate matter and total column aerosol depth, in prep., 2016.

1109   Wexler, A. S., and Clegg, S. L.: Atmospheric aerosol models for systems including the ions H+, NH4+, Na+,

Atmospheric
Chemistry
and Physics
Discussions
Open Access
EGU

1110   SO42−, NO3−, Cl−, Br−, and H2O, J. Geophys. Res. Atmos., 107(D14), ACH14–1–14,
1111   doi:10.1029/2001JD000451, 2002.

1112   WHO: Human exposure to air pollution, in Update of the World Air Quality Guidelines World Health Organization,
1113   pp. 61–86, World Health Organization, Geneva, Switzerland., 2005.

1114   WHO: WHO | Air quality guidelines - global update 2005, World Health Organization, Geneva, Switzerland., 2006.

1115   Wise, M. E., Surratt, J. D., Curtis, D. B., Shilling, J. E., and Tolbert, M. A.: Hygroscopic growth of ammonium
1116   sulfate/dicarboxylic acids, J. Geophys. Res. Atmos., 108(D20), 4638, doi:10.1029/2003JD003775, 2003.

1117   Yang, F., Tan, J., Zhao, Q., Du, Z., He, K., Ma, Y., Duan, F., and Chen, G.: Characteristics of $PM_{2.5}$ speciation in
1118   representative megacities and across China, Atmos. Chem. Phys., 11(11), 5207–5219, doi:10.5194/acp-11-5207-
1119   2011, 2011.

1120   Zhang, R., Jing, J., Tao, J., Hsu, S.-C., Wang, G., Cao, J., Lee, C. S. L., Zhu, L., Chen, Z., Zhao, Y., and Shen, Z.:
1121   Chemical characterization and source apportionment of $PM_{2.5}$ in Beijing: seasonal perspective, Atmos. Chem. Phys.,
1122   13(14), 7053–7074, doi:10.5194/acp-13-7053-2013, 2013.

1123   Zhang, W.-J., Sun, Y.-L., Zhuang, G.-S., and Xu, D.-Q.: Characteristics and seasonal variations of PM2.5, PM10,
1124   and TSP aerosol in Beijing, Biomed. Environ. Sci., 19(6), 461–468, 2006.

1125

1126

Atmospheric
Chemistry
and Physics
Discussions

1127 **Figures and Tables**

1128
1129 **Table 1: κ-Kohler constants for volume (κ_v), mass (κ_m), and related quantities**

Compound [X]	$\kappa_{v,X}$	Approximate Density (ρ_X/ρ_{water})	$\kappa_{m,X}$	PBW(%mass) at RH = 35%	RH = 80%
Crustal	0	2.5[a]	0	0	0
EBC	0	1.8[b]	0	0	0
TEO	0	2.5	0	0	0
RM	0.1[c]	1.4	0.07	2	12
ANO$_3$	0.41	1.72	0.24	17	61
ASO$_4$	0.51	1.76	0.29	15	56
Na$_2$SO$_4$	0.68[d]	2.68[d]	0.25	12	50
NaCl	1.5[e]	2.16	0.69	22	68

1130 PBW = Particle-bound water. EBC = Equivalent black carbon, TEO = Trace Element Oxides, RM = Residue Matter
1131 (associated with organics), ANO$_3$ = ammonium nitrate, ASO$_4$ = ammonium sulfate. [a] Wagner et al. (2009), [b]Bond
1132 and Bergstrom (2006), [c]Assuming an urban O:C ratio of 0.5 then $\kappa_{v,OM} = 0.1$ Jimenez et al. (2009), [d]Petters and
1133 Kreidenweis (2007). [e]Fitted using non-deliquesced, subsaturated AIM Model III values, plus 0% RH endpoint by
1134 Kreidenweis et al. (2008).

1135
1136
1137
1138 **Table 2: Summary of speciation definitions**

Species (at 0% RH)	Measurement Method	Species Mass (µg). For concentrations, divide masses by sampling volume v	Reference
NaCl	IC (anion and cation)	$[Na^+]_{SS} = [Na^+]_{tot} - 0.1[Al]$ $2.54[Na^+]_{SS}$	(Remoundaki et al., 2013) (Malm et al., 1994)
ANO$_3$		$1.29[NO_3^-]$	(Malm et al., 1994)
ASO$_4$		$[SO_4^{2-}]_{non-ss} + [NH_4^+] - 0.29[NO_3^-]$ where $[SO_4^{2-}]_{non-ss} = [SO_4^{2-}]_{total} - 0.12[Na^+]$	(Dabek-Zlotorzynska et al., 2011; Henning et al., 2003)
Na$_2$SO$_4$		$0.18[Na^+]_{SS}$	
CM	ICP-MS & IC	$([Al] + [Mg] + [Fe])/0.1$	(Wang, 2015)
EBC	SSR	$20.7 \times \ln(R_o/R)$	(Taha et al., 2007)
TEO	ICP-MS	$1.47[V] + 1.27[Ni] + 1.25[Cu] + 1.24[Zn] + 1.32[As] + 1.2[Se] + 1.07[Ag] + 1.14[Cd] + 1.2[Sb] + 1.12[Ba] + 1.23[Ce] + 1.08[Pb]$	(Malm et al., 1994)
PBW$_{inorg}$	$\kappa_{m,X}$	$\sum_X [f_{m,X}(RH) - 1][X]$	(Kreidenweis et al., 2008)
PBW$_{RM}$		$RM(1 - 1/f_{m,RM})$	Table 1
RM(35%)	Mass Balance	$[PM_{2.5}] - \{[EBC] + [CM] + [TEO] + [ANO_3] + [NaCl] + [ASO_4] + [Na_2SO_4] + [PBW_{inorg}]\}$	This Study
RM(0%)	Mass Balance $\kappa_{m,OM} = 0.07$	$RM(35\%) - PBW_{RM}$	Organic growth factors: (Jimenez et al., 2009; Sun et al., 2011)

1139 **Species**: EBC = Equivalent black carbon, TEO = Trace metal oxides, CM = Crustal Material, ANO$_3$ = Ammonium
1140 nitrate, ASO$_4$ = Ammonium sulfate, PBW = particle-bound water, RM = residue matter (assumed representative of
1141 organic matter). **Measurement Instruments:** IC = Ion Chromatography, ICP-MS Inductively coupled plasma mass
1142 spectrometry, $\kappa_{m,X}$ = single-parameter hygroscopicity by mass (Kreidenweis et al., 2008).

1143

Atmospheric
Chemistry
and Physics
Discussions

Table 3: PM$_{2.5}$ composition and water content (μg m^{-3}) at each SPARTAN location.

City	Host Institute	Lat/Lon (°)	Elev.//Inst. Elev. (m)	Filters (n)	ASO$_4$	ANO$_3$	CM	NaCl	EBC	TEO	RM	PBW 35%RH	ρ 0%RH (g/cm³)	PM$_{2.5}$	PM$_{2.5}$/PM$_{10}$	κ$_{v,tot}$	PM$_{2.5}$ Zn/Al	Filter Sampling Period
Beijing	Tsinghua University	40.010, 116.333	60// 7.5	100	12.0 (7.6)[a]	4.7 (5.8)	13.4 (7.1)	1.3 (2.1)	5.6 (3.6)	0.62 (0.32)	28.4 (19.5)	4.7 (2.4)	1.64	67.9 (2.6)	0.48	0.19	0.45	2013/06 – 2015/10
Bandung	ITB Bandung	-6.888, 107.610	826// 20	71	6.0 (2.3)	0.5 (0.4)	2.4 (1.2)	0.3 (0.1)	3.9 (2.0)	0.17 (0.10)	15.5 (5.6)	1.9 (0.6)	1.56	30.6 (1.0)	0.58	0.17	0.53	2014/01 – 2015/09
Manila	Manila Observatory	14.635, 121.080	60// 10	56	2.7 (1.5)	0.3 (0.2)	1.8 (1.2)	0.4 (0.2)	4.3 (3.3)	0.12 (0.10)	7.4 (3.6)	1.0 (0.4)	1.61	17.9 (0.9)	0.39	0.15	0.89	2014/02 – 2015/09
Dhaka	Dhaka University	23.728, 90.398	20// 20	41	7.5 (4.3)	2.1 (1.8)	6.7 (3.2)	1.4 (1.7)	8.0 (6.2)	1.50 (1.46)	21.1 (14.9)	3.5 (2.1)	1.64	51.9 (3.7)	0.4	0.17	2.68	2014/05 – 2015/11
Ilorin	Ilorin University	8.484, 4.675	330// 10	40	1.9 (0.8)	0.3 (0.1)	2.8 (1.8)	0.3 (0.4)	1.6 (0.8)	0.11 (0.07)	7.8 (3.9)	0.9 (0.4)	1.61	15.7 (0.8)	0.44	0.15	0.53	2014/03 – 2015/10
Kanpur	IIT Kanpur	26.519, 80.233	130// 10	33	17.3 (11.8)	6.7 (5.3)	4.2 (3.0)	0.6 (0.3)	8.1 (4.7)	0.62 (0.47)	53.3 (33.9)	6.2 (3.6)	1.52	97.2 (9.2)	0.56	0.18	1.36	2013/12 – 2014/11
Buenos Aires	CITEDEF	-34.560, -58.506	25// 7	21	1.1 (0.3)	0.8 (0.7)	2.2 (0.8)	0.6 (0.3)	1.1 (1.3)	0.12 (0.12)	2.7 (2.3)	0.9 (0.3)	1.72	10.0 (0.6)	0.37	0.20	0.42	2014/10 – 2015/04
Mammoth Cave NP	Mammoth Cave	37.132, -86.148	235// 7	19	4.1 (2.4)	0.2 (0.1)	1.4 (1.3)	0.1 (0.1)	0.7 (0.4)	0.03 (0.02)	6.3 (4.5)	1.0 (0.6)	1.58	13.6 (1.8)	0.56	0.22	0.13	2014/06 – 2014/08
Rehovot	Weizmann Institute	31.907, 34.810	20// 10	19	4.8 (1.6)	0.7 (0.4)	2.1 (0.5)	0.9 (0.6)	2.0 (2.4)	0.09 (0.05)	2.7 (3.0)	1.7 (0.7)	1.73	15.2 (1.3)	0.41	0.31	0.59	2015/02 – 2015/08
Atlanta	Emory University	33.688, -84.290	250// 2	13	2.0 (0.9)	0.3 (0.1)	0.9 (0.4)	0.1 (0.1)	0.9 (1.0)	0.04 (0.02)	4.1 (1.8)	0.6 (0.2)	1.63	9.1 (0.7)	0.69	0.17	0.31	2014/01 – 2014/05
Hanoi	Vietnam Acad. Sci.	21.048, 105.800	10// 20	10	6.0 (2.1)	1.6 (0.4)	6.1 (4.6)	0.9 (0.2)	3.7 (2.1)	0.70 (0.37)	17.8 (7.7)	2.6 (0.7)	1.59	39.4 (3.9)	0.38	0.18	2.57	2015/05 – 2015/08
Singapore	NUS	1.298, 103.780	10// 20	6	17.6 (7.3)	1.5 (1.2)	2.4 (0.5)	1.1 (0.4)	2.4 (1.4)	0.22 (0.06)	39.8 (27.2)	5.5 (2.6)	1.51	70.6 (16.2)	0.77	0.21	1.57	2015/08 – 2015/09
Pretoria	CSIR	-25.756, 28.280	1310// 10	5	1.2 (1.6)	0.7 (0.3)	1.4 (1.6)	0.2 (0.1)	1.4 (0.9)	0.07 (0.04)	0.9 (0.7)	0.5 (0.4)	1.97	6.4 (2.3)	0.32	0.29	0.69	2015/09- 2015/11
SPARTAN mean (% mass)	All sites			437	20 (10)%	4.0 (2.8)%	11.9 (6.2)%	2.2 (1.5)%	10.7 (8.4)%	0.85 (0.63)%	43 (25)%	7.2 (3.1)%	1.61	35.2 (3.6)	0.49	0.194	0.69	**2013 – 2015**

[a]Values in parentheses are 1σ standard deviations. ANO$_3$ = ammonium nitrate, ASO$_4$ = ammonium sulfate, CM = Crustal material, EBC = Equivalent black carbon, TEO = Trace Element Oxides, RM = Residue Matter, PBW = Particle-bound water. Mean Na$_2$SO$_4$ was not significant (< 0.1 μg m^{-3}) at any SPARTAN site. [b]Geometric mean of ratio

Atmospheric
Chemistry
and Physics

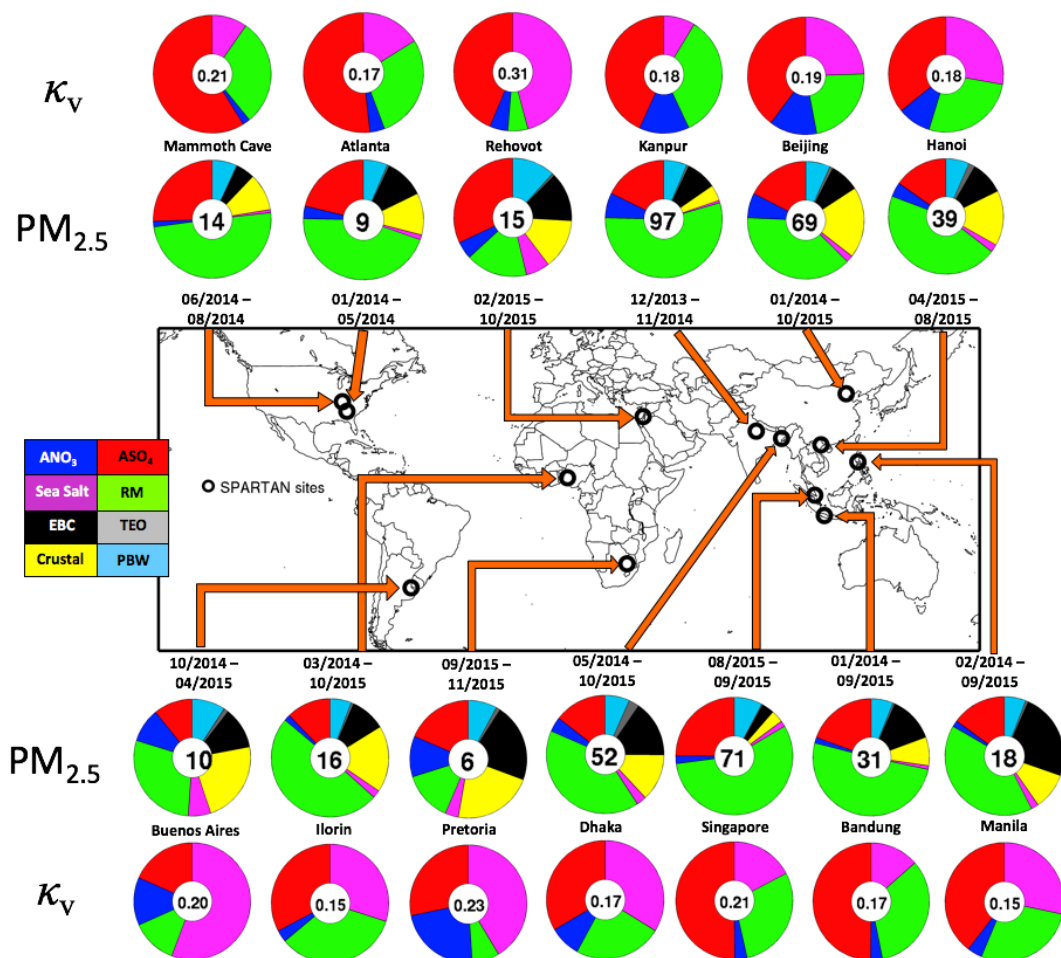Open Access

Discussions

EGU

Figure 1: PM$_{2.5}$ mass (inner circle, μg m^{-3}) and composition mass fraction (filled colors) is shown in interior pie charts. Exterior pie charts contain site-mean κ_ν surrounded by the relative contribution of PBW water at 35% RH.
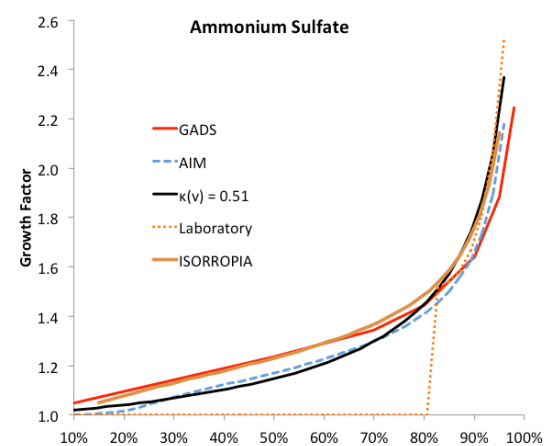
Figure 2: Hygroscopic growth factors for ASO$_4$ (left), ANO$_3$ (centre), and sea salt (right). GADS = Global Aerosol Dataset estimated from empirical data (Koepke et al., 1997)**. ISORROPIA = Aerosol thermodynamic model at T=298K (reverse mode) and assuming linear water/solvent volume additivity** (Fountoukis and Nenes, 2007)**. AIM = Aerosol Inorganic Model calculated metastable growth for ASO$_4$ and ANO$_3$ at T=298K** (Wexler and Clegg, 2002)**, Laboratory ASO$_4$ fit is $GF = 1.49 + 2.81 \cdot RH^{24.6}$ (with deliquescence at 80%) is for bulk pure ASO$_4$** (Wise et al., 2003)**. All components are fit using Eq 3.**
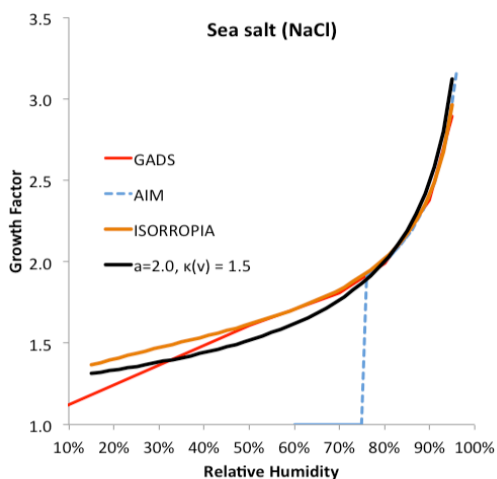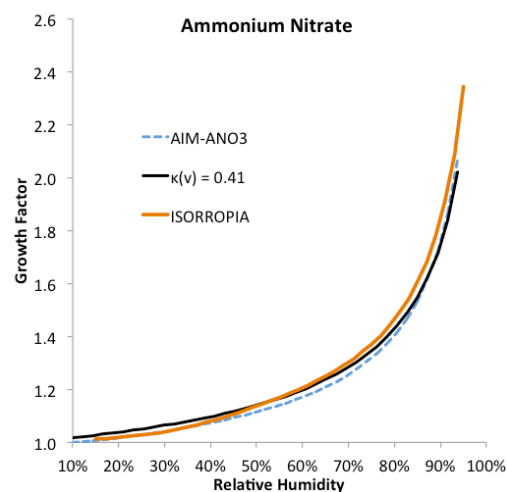
Atmospheric
Chemistry
and Physics
Discussions

Figure 3: Comparison of SPARTAN water-free aerosol composition with 11 collocated speciation studies. The numbers in parentheses show 1-σ deviations of averaged masses. The number of filters sampled is *n*. Dark green = organic, Light green = residue, black = equivalent black carbon, red = ammonium sulfate, blue = ammonium nitrate, purple = sea salt, yellow = crustal, and grey stripes = unknown. OM/OC ratios are from Philip et al. (2014b) and Canagaratna et al. (2015). Relative mass percentages are based on water-free aerosol components. SPARTAN percentages do not sum to 100% due to omission of species not found in comparison studies.

$PM_{2.5}$ mass = μg m^{-3} (1σ/√n), components = % (1σ)		
This study (total mass = μg m^{-3})	**Study A (μg m^{-3})**	**Study B (μg m^{-3})**

Beijing $PM_{2.5}$: 70 (3), *n* = 100

7 (9)% ANO$_3$,
19 (12)% ASO$_4$,
2.1 (3.5)% NaCl,
21 (11)% CM,
9.0 (3.5)% EBC,
42 (30)% RM

(Yang et al., 2011) 2005-2006,
OM/OC = 1.7, $PM_{2.5}$: 119(40)

11 (7)% ANO$_3$,
17 (10)% ASO$_4$,
1.3 (0.6)% NaCl,
19 (3)% CM,
7 (5)% EC,
33 (16)% OM,
10 (10)% Unk

(Oanh et al., 2006) 2001-2004,
OM/OC = 1.7 $PM_{2.5}$: 136 (45)

12 (1.5)% ANO$_3$,
20 (1.8)% ASO$_4$,
1.2 (1.2)% NaCl,
5 (3)% CM,
9 (7)% EBC,
29 (22)% OM,
24 (24)% Unk

Bandung $PM_{2.5}$: 31 (1), *n* = 71

1.8 (1.4)% ANO$_3$,
20 (8)% ASO$_4$,
1.1 (0.4)% NaCl,
8.4 (4.2)% CM,
14 (4)% EBC,
54 (20)% RM

(Oanh et al., 2006) 2001-2004.
OM/OC = 2.2, $PM_{2.5}$: 45.5(10.6),

13(4)% ANO$_3$,
21(3)% ASO$_4$,
1.6(0.2)% NaCl,
6.6(0.5)% CM,
19 (4)% EBC,
36(11)% RM

(Lestari and Mauliadi, 2009) 2001- 2007, OM/OC = 2.2 $PM_{2.5}$: 43.5(10.5)

4(6)% ANO$_3$,
4(4)% ASO$_4$,
3(2)% NaCl,
23(21)% CM,
24(14)% EBC,
42(35)% RM

Manila $PM_{2.5}$: 18 (1), *n* = 56

1.8 (1.2)% ANO$_3$,
16 (9)% ASO$_4$,
2.4 (1.2)% NaCl,
11 (3)% CM,
25 (12)% EBC,
44 (22)% RM

(Cohen et al., 2009) 2001-2007,
OM/OC = 2.1, $PM_{2.5}$: 46 (19),

ANO$_3$ N/A
14 (9)% ASO$_4$,
0.6 (1.5)% NaCl,
5 (1.7)% CM,
25 (11)% EBC,
57(22)% OM,

Kanpur $PM_{2.5}$: 97 (9), *n* = 33

7.4 (6.7)% ANO$_3$,
19 (15)% ASO$_4$,
0.7 (0.3)% NaCl,
4.7 (2.9)% CM,
9 (5.0)% EBC,
59 (50)% RM

(Behera and Sharma, 2010) Oct. 2007 – Jan 2008,
OM/OC = 2.2, $PM_{2.5}$: 172 (73),

6.1 (1.3)% ANO$_3$,
18 (4)% ASO$_4$,
2.6 (0.6)% NaCl,
10 (3)% CM,
4.8 (1.1)% EC,
42 (9)% OM,
16 (10)% Unk

(Ram et al., 2012) Dec 2008 – Feb 2009,
OM/OC = 2.2 $PM_{2.5}$: 158 (47)

6.6(4)% ANO$_3$,
13 (5)% ASO$_4$,
1.5 (0.9)% NaCl,
12 (6)% CM*,
3 (1.1)% EC,
57 (23)% OM,
6 (24)% Unk

*Assuming CM = [Ca]/0.034 (Wang, 2015)

Mammoth Cave NP $PM_{2.5}$: 13.6 (2), *n* = 19

1.1 (0.9)% ANO$_3$,
30 (14)% ASO$_4$,
0.6 (0.8)% NaCl,
10 (10)% CM,
4.0 (2.5)% EBC,
47 (40)% RM

(IMPROVE, 2015) June-Aug. 2014,
OM/OC = 2.0, $PM_{2.5}$: 10.0 (5.8),

2.4 (2.5)% ANO$_3$,
36 (17)% ASO$_4$,
0.3 (1.6)% NaCl,
7 (8)% CM,
3 (3)% EC,
34 (30)% OM,
17% Unk+H$_2$O

Atlanta $PM_{2.5}$: 9.1 (1), *n* = 13

3.6 (1.3)% ANO$_3$,
24 (12)% ASO$_4$,
1.2 (1.3)% NaCl,
11 (6.6)% CM,
11 (2.6)% EBC,
49 (25)% RM

(Butler et al., 2003) Mar. 1999 –2000 Feb,
OM/OC = 2.0, $PM_{2.5}$: 24.2

4 (0.2)% ANO$_3$,
28 (1.0)% ASO$_4$,
10 (0.8)% CM,
3 (0.2)% EC,
55 (5)% OM,

EPA 2007 –2013 (USEPA, 2015), OM/OC = 2.0
$PM_{2.5}$: 15.3

5.0 (5)% ANO$_3$,
21 (15)% ASO$_4$,
0.6 (0.6)% NaCl,
7.3 (5)% CM,
7.2 (5)% EC,
60 (36)% OM,

Hanoi
$PM_{2.5}$: 39 (4), *n* = 10

4.4 (1.1)% ANO$_3$,
17 (6)% ASO$_4$,
2.5 (0.6)% NaCl,
17 (13)% CM,
10 (3.3)% EBC,
49 (21)% RM

(Cohen et al., 2010). 2001 –2008
OM/OC = 2.1, $PM_{2.5}$: 54 (33)

ANO$_3$ N/A
29 (20)% ASO$_4$,
0.6 (1.4)%NaCl
13 (7)% CM,
8 (3)% EBC,
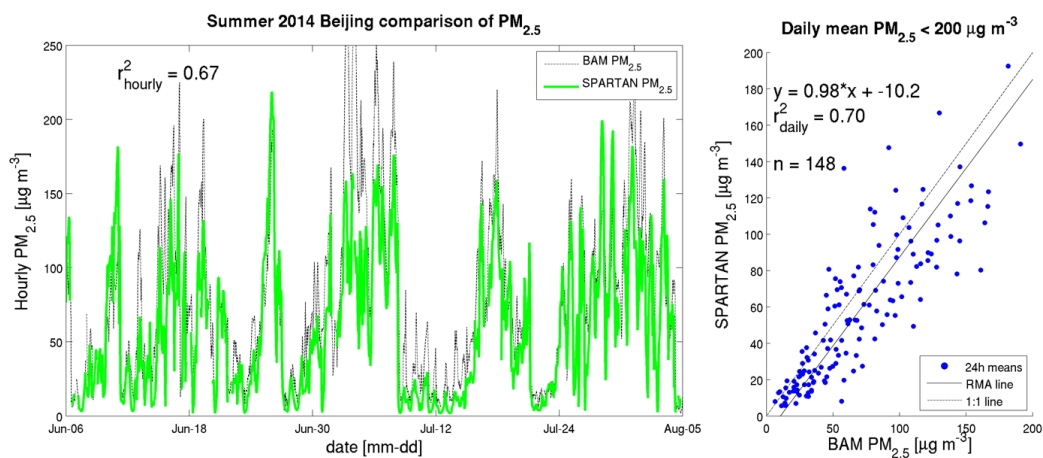40 (19)% OM,
2 (2)% Unk + ANO$_3$

Figure 4: Left Hourly PM$_{2.5}$ estimated from SPARTAN overlaid with a MetOne BAM-1020 (June-August 2014) at the Beijing US Embassy (15 km away). Right: 24-hour PM$_{2.5}$ predictions compared with BAM for the year 2014. Reduced major axis (RMA) slope and Pearson correlations for PM$_{2.5}$ are given in inset.

Atmospheric
Chemistry
and Physics

Discussions

Appendix:

Appendix A1:

Table A1: Hygroscopicity parameter κ_v for various studies on organic material

κ_v (OM)	Comments	Reference
0.045	Fitted to an aged organic mixture, subsaturated	(Varutbangkul et al., 2006)
0	IMPROVE network, subsaturated	(Hand and Malm, 2006)
0.10 ± 0.04	RH > 99%, fitted to SOA precursors	(Prenni et al., 2007)
$-0.067 + 0.33$(O:C)	Fitted, RH > 99%	(Jimenez et al., 2009)
0.29(O:C)	RH > 99%, 0.3 < O:C < 0.6	(Chang et al., 2010)
0.05	Best estimate from aged mixtures, subsaturated	(Dusek et al., 2011)
0.01 – 0.2	Field studies & smog chamber, subsaturated	(Duplissy et al., 2011)
0.16	RH > 99%	(Asa-Awuku et al., 2011)
0.05 – 0.13	Lab experiments, aged with H_2O_2 and light; subsaturated	(Liu et al., 2012)
0.1	RH > 99%, D_{dry} < 100 nm	(Padró et al., 2012)
$0.12\varepsilon_{WSOM}$[#]	RH > 99%	(Lathem et al., 2013)
$-0.005 + 0.19$(O:C)	Fitted, RH > 99% 100 nm particle	(Rickards et al., 2013)
0.03, 0.1	HDTMA-measure, subsaturated	(Bezantakos et al., 2013)
0.1	Subsaturated	Selected for this study

[#]ε_{WSOM} = fraction of water-soluble organic material.

Appendix A2:

Dry aerosol scatter ($b_{sp,\text{dry}}$) is related to relative humidity (RH) by

$$b_{sp,\text{dry}} = \frac{b_{sp}(\text{RH})}{f_v(\text{RH})} \qquad \text{Eq. A1}$$

Changes in scatter are also proportional to mass (Chow et al., 2006; Wang et al., 2010)

$$b_{sp,\text{dry}} = \alpha \text{PM}_{2.5,\text{dry}} \qquad \text{Eq. A2}$$

where α (m^2 g^{-1}) is the mass scattering efficiency and a function of aerosol size distribution, effective radius, and dry composition. In this study we treat composition, density, and size distribution as constant over each of our 9-day intermittent sampling periods so that $\alpha \approx \langle \alpha \rangle_{9d}$. Under this assumption the predicted mass changes in low humidity (35% RH) are proportional to water-free aerosol scatter:

$$\text{PM}_{2.5,\text{dry}} = \langle \text{PM}_{2.5,\text{dry}} \rangle \frac{b_{sp,\text{dry}}}{\langle b_{sp,\text{dry}} \rangle} \qquad \text{Eq. A3}$$

where $< >$ indicates 9-day averages. The explicit compensation for aerosol water is then

$$[\text{PM}_{2.5,\text{dry}}] = \frac{\langle [\text{PM}_{2.5,\text{dry}}] \rangle}{\langle b_{sp}(\text{RH})/f_v(\text{RH}) \rangle} \cdot \frac{b_{sp}(\text{RH})}{f_v(\text{RH})} \qquad \text{Eq. A4}$$

where [] indicates concentration in μg m^{-3}. Uncertainties are a function of replicate weighing measurements (± 2 μg), flow volume (± 10%), %RH (± 2.5), aerosol scatter (± 5%), and κ$_v$ (± 0.05).

$$\left(\frac{\delta [\text{PM}_{2.5,h}]}{[\text{PM}_{2.5,h}]} \right)^2 \approx \left(\frac{\delta \text{PM}_{2.5}}{\text{PM}_{2.5}} \right)^2 + \left(\frac{\delta V}{V} \right)^2 + \left(\frac{\delta b_{sp}}{b_{sp}} \right)^2 + \left(\frac{\delta f_v}{f_v} \right)^2 \qquad \text{Eq. A5}$$

where

$$\left(\frac{\delta f_v}{f_v} \right)^2 = \frac{(f_v - 1)^2}{f_v^2} \left[\left(\frac{\delta \kappa}{\kappa} \right)^2 + \left(\frac{\delta \text{RH}}{\text{RH} \cdot (100 - \text{RH})} \right)^2 \right] \qquad \text{Eq. A6}$$

The average relative 2-σ PM$_{2.5}$ uncertainty was 26% for dry hourly predictions, increasing with higher RH cutoffs. A cut-off of RH = 80% has been applied to our data, above which hygroscopic uncertainties, as well as total water mass, dominate.